Reply to Anonymous Referee 1:

We would like to thank the reviewer for taking time to review this manuscript thoroughly and for their comprehensive comments received. We have addressed all comments in turn below:

Specific comments:

1. Please provide details of the global model and resolution of the data which is used for the forcing?

The SAMBBA LAM was driven by the global NWP GA3.1 configuration of the Met Office Unified Model (Walters et al., 2011) with a horizontal resolution of N512 (25km) and 70 vertical levels with the model lid at 80km References:

D.N. Walters, M.J. Best, A.C. Bushell, D. Copsey, J.M. Edwards, P.D. Falloon, C.M. Harris, A.P. Lock, J.C. Manners, C.J. Morcrette, M.J. Roberts, R.A. Stratton, S. Webster, J.M. Wilkinson, M.R. Willett, I.A. Boutle, P.D. Earnshaw, P.G. Hill, C. MacLachlan, G.M. Martin, W. Moufouma-Okia, M.D. Palmer, J.C. Petch, G.G. Rooney, A.A. Scaife, and K.D.Williams, The Met Office Unified Model Global Atmosphere 3.0/3.1 and JULES Global Land 3.0/3.1 configurations, Geosci. Model Dev., 4, 919-941, 2011.

We have added,

"*Meteorological boundary conditions for all runs (3 hourly) are provided by the global operational NWP model (global GA3.1 configuration of the UK at N512 (25 km); Walters et al., 2011). In the PROG, the BBA is free-running for two days, with spin-up of BBA from the beginning of August.*"

to the paper text.

2. Did you assimilate any data using 3DVar on the global forcing? If it is the case, which data should be assimilated?

The global model is initialised using a continuous 6-hourly cycle of four-dimensional variational data assimilation (4D-Var) (Rawlins et al., 2007). But the LAM itself has its own 6 hourly 3D VAR assimilation (Lorenc et al. 2000) where the u, v winds, potential temperature, density, pressure, and moisture variables are assimilated on a 6 hourly cycle. In the runs we analyse in this paper, the 2 day 00Z forecast is spun up from an assimilated start dump and then free running and is forced 3 hourly at the boundaries by the global model forecasts.

Rawlins, R., Ballard, S., Bovis, K., Clayton, A., Li, D., Inverarity,

G., Lorenc, A., and Payne, T.: The Met Office global fourdimensional

variational data assimilation scheme, Q. J. Roy. Meteorol.

Soc., 133, 347–362, doi:10.1002/qj.32, 2007.

3. Did you considered the spin up time for the model, when you considered the 48 hr forecast?

The prognostic aerosol in the two-day forecasts are initialised rather than being a "cold-start". The forecast chain was spun-up from the beginning of August, which is more than enough time to spin-up the modelled aerosol.

4. CLIM performance is not well captures the phenomena's as compared to PROG simulations at all the observational sites, what is the initial and boundary conditions is used for the CLIM simulations??

All the simulations such as NOA, PROG and CLIM have the same initial and boundary conditions driven by global UM model. Any differences between NOA, PROG and CLIM are due to their different representations of the aerosol.

5. Page 18894, line -27: Please mention the level of aerosol layer?

Fig. 6a shows aerosol layer up to 500hPa. We have included in the revised manuscript (MS).

"500hPa"

6. Page 18896, line-11: " The inclusion of aerosols improves the surface temperatures biases at T +12 and T + 24 h". It would be great if you could explain about the comment.

Figure 9 in the MS shows a verification plot of model error and RMSE in surface temperature against ground observations for the SAMBBA period as a function of forecast lead time. The aerosols (i.e. PROG or CLIM compared with NOA) generally improve the surface temperature biases and reduce RMSEs, most notably at S3 and S4. This is in fact not only at T+12 and T+24 so we now state,

"*The inclusion of aerosols tends to improve the surface temperatures biases in forecasts*"

Technical comments

In page No. 18893, line No.5: Please check whether word 'a' before 'around' is meaningful??

We removed in the revised MS.

In page No.18894, line no. 5: Please remove surface word which is written twice

We removed as suggested by Reviewer 1 and 3 in the revised MS.

Anonymous Referee #2

We would like to thank the reviewer for taking time to review this manuscript thoroughly and for their comprehensive comments received. We have addressed all comments in turn below:

Comments: 1) I might be wrong, but I am not completely confident about the experimental setting: the PROG includes prognostic BBA while all the other aerosols are climatological. The difference with NOA (no aerosols at all) is thus not due only to BBA (I understand that BBA represent a large contribution to the AOD of the region (P18885), but there are other contributors too), hence the statement at P18890 L15 (and following analysis where the difference PROG-NOA is attributed to BBA aerosols) seems not completely correct.

We appreciate reviewer comment that the impacts contributed not only from BBA aerosols but also other aerosols. We have included statement that "*Impacts of other aerosols contributions are small in the Amazonia region during the SAMBBA period***" which can be seen in the revised Fig.2 (labelled contour values show BBA AODs). In addition, the figure below presents the ratio of BBA aod to other aerosols AOD's: other aerosols such as sea salt, sulphate, mineral dust, soot and fossil fuel contribution from models are small i.e. contribute about 6 to 16% of AODs over Amazonia.**

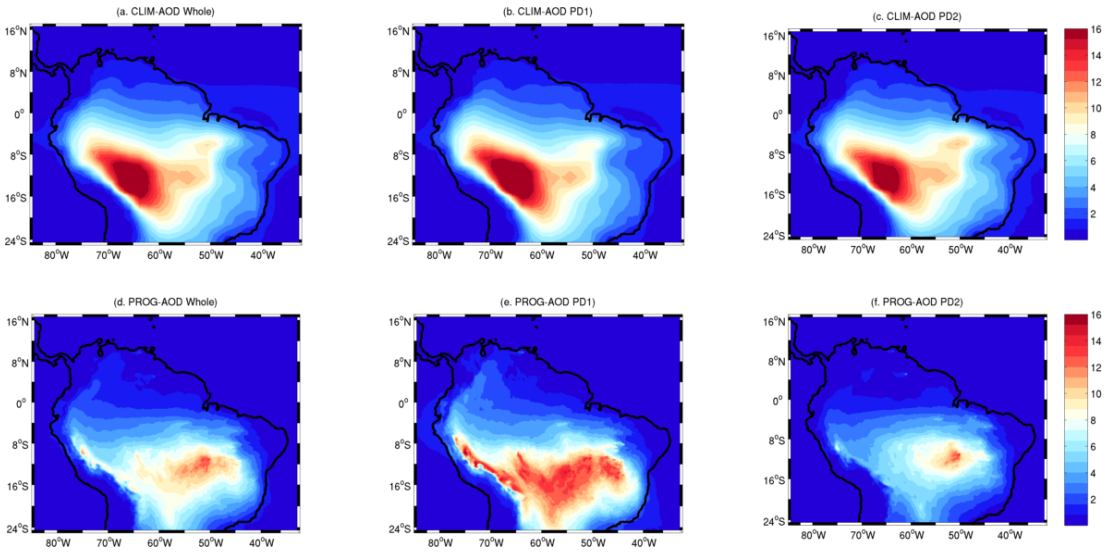

Modelled ratio of BBA AOD to AOD from other species (sulphate+mineral dust+sea salt+soot+fossil fuel). PD1 is period 1, PD2 is period 2, Whole is for whole period. Top row shows CLIM and lower row PROG.

2) Add significance test (e.g., masking out not significant areas) in the geographical maps (Figs. 2, 4, 5, etc.)

We have added contours of significance in Figs. 4, 5 and 6b. Since the only differences between the 3 models is their representation of aerosol, we have a clear chain of cause-and-effect from aerosol through radiation to meteorology. Values on plots are therefore informative, even where they are not statistically significant. We have therefore contoured the significant regions, instead of masking out the non-significant values. We cannot do this on Figure 2 as this is of model means states, rather than of differences. *We have calculated the significant values using the Standard Error (SE) using the following method (please note that autocorrelation has been accounted for in the time series of each pixel):*

$SE = (SD/\sqrt{N}) * k$

where "SD" is the standard deviation and "N" is the number of points (i.e. how many times contribute to each pixel in the model domain). "k" is the autocorrelation correction factor. This is based on the J.R. Bence (1995).

$k=[(1+p)/(1-p)]^{0.5}$

where "p" is the autocorrelation function. "p" is calculated using the Prais-Winsten estimation (see Bence, (1995) – included in reference list) .

We have contoured the values where the SEs are greater than the absolute difference.

3) How representative is the specific period investigated compared to climatological

mean conditions?

Mean AODs from MODIS are presented in the figure below. All plots are for the model simulation duration (14 Sept to 03 October, towards the end of the dry season when AODs from BBA are high). The figure shows significant year-to-year variations in AODs and that 2012 is a below average year. This is now noted in the paper,

We have added

"We also expect BBA impacts to be greater in an average year, when compared with 2012, which had lower than average AOD values (i.e. approximate half the size)."

to the paper text.

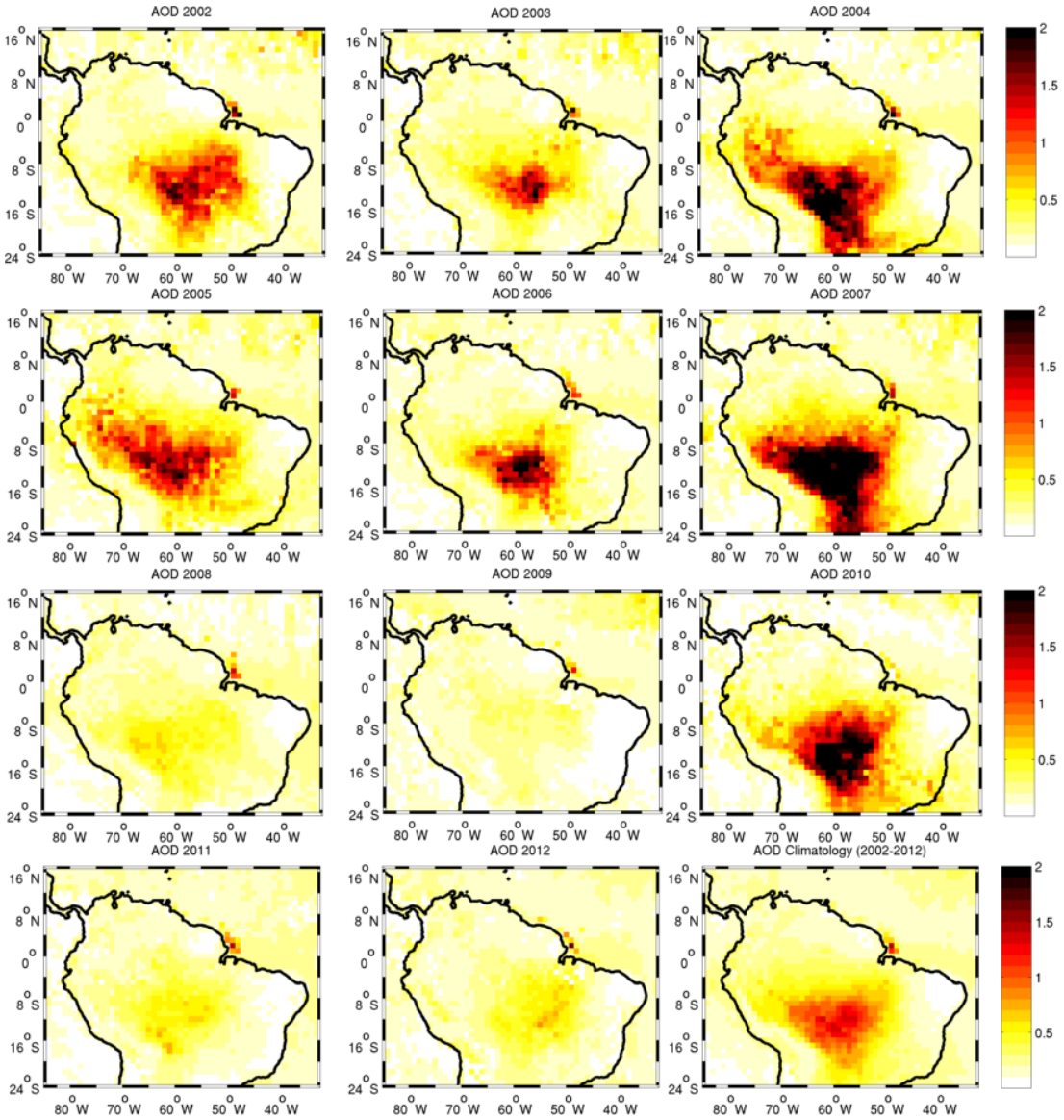

4) Fig. 2: it would be helpful to plot BBA AOD as contours.

We thank to Reviewer for suggestion. We overplotted labelled BBA AOD contours in the revised manuscript (MS).

4) P18885, L11: what are the "total" emissions?

Emissions of BC from different sources such as on road mobile sources (i.e. diesel sources), biomass burning and domestic BC emissions. We have deleted the word 'total' to avoid confusion

5) P18893, L23: how do you infer that these changes are due to clouds?

The changes in 2-m temperature are consistent with changes in whole-sky radiation (below) and the differences between clear-sky and whole-sky radiation are due to clouds. In addition the changes are too unevenly distributed for it to be likely that they are from changes in advection.

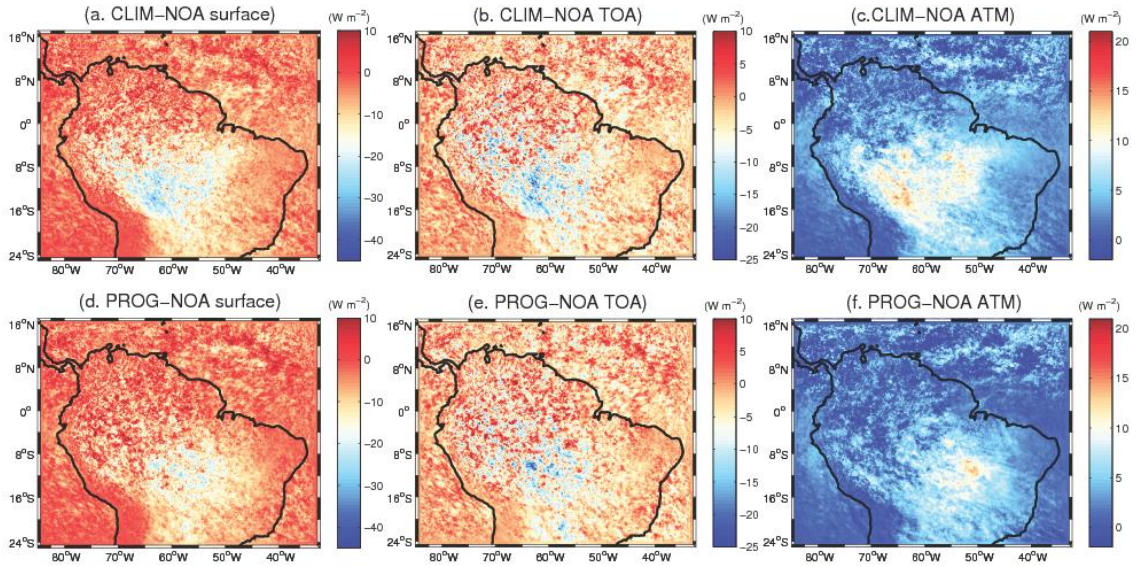

Impact of (top row) CLIM and (bottom row) PROG aerosol representations on (a, d) the net surface radiation, (b, e) net TOA radiation, (c, f) net atmospheric divergence averaged over the whole SAMBBA period for the whole-sky.

6) P18899, L25: which variables are assimilated?

The global model is initialised using a continuous 6-hourly cycle of four-dimensional variational data assimilation (4D-Var) (Rawlins et al., 2007). But the LAM itself has it's own 6 hourly 3D VAR assimilation (Lorenc et al. 2000) where the u, v winds, potential temperature, density, pressure, and moisture variables are assimilated on a 6 hourly cycle. In the runs we analyse in this paper, the 2 day 00Z forecast is spun up from an assimilated start dump and then free running and is forced 3 hourly at the boundaries by the global model forecasts.

7) Fig. 6: could you explain the motivation for choosing this area?

We choose the maximum AOD loading region (Fig.2) to see the maximum impacts. Hence we took the 10-13^{o}S latitudinal average.

7) Fig. 11: mask out values around 0

We have masked out values in the revised manuscript.

8) Language improvements: P18887, L3: tropospheric P18887, L4: weakened

P18887, L14: provided by P18893, L5: between 10 and 20 P18893, L7: for the whole

period P18893, L11: scales of one degree

We thank to reviewer for language improvements help. We have made all suggested changes in the revised MS. Please see them in bold format.

Anonymous Referee #3

We would like to thank the reviewer for taking time to review this manuscript thoroughly and for their comprehensive comments received. We have addressed all comments in turn below:

Specific comments:

Page 18884, Lines 23-24: It is stated that inclusion of biomass burning aerosols in the MetUM model significantly improves the forecast of temperature and relative humidity. However, we don't see any substantial reduction in mean bias and RMSE (Figs. 9 and 10) due to inclusion of biomass burning aerosols in the model. The bias in relative humidity even increases above 700 hPa when the model is used with a prognostic aerosol scheme. In view of this, I suggest removing this line from the abstract. Could you also please examine the statistical significance of aerosol induced changes in the meteorological parameters reported in this paper?

We have clarified this statement by stating,

"*Inclusion of climatological or prognostic BBA in the MetUM makes a small but significant improvement in forecasts of temperature and relative humidity*". **To support this statement, Figure 9 shows how CLIM or PROG tends to reduce bias and RMSE, now clarified in the text as,** *"The inclusion of aerosols tends to improve the surface temperatures biases in forecasts"***. In addition we have tested the significance of the difference between mean correlations between models and observations at S1-4 (shown below, with correlation values shown). PROG and CLIM are significantly better correlated with the observations than NOA at the 99% level as stated in the paper at line 18, page 18899. Furthermore we have now added contours to Figs 4, 5 and 6b, to show where differences due to aerosols are statistically significant, using a method Bence, (1995) that accounts for auto-correlation**.

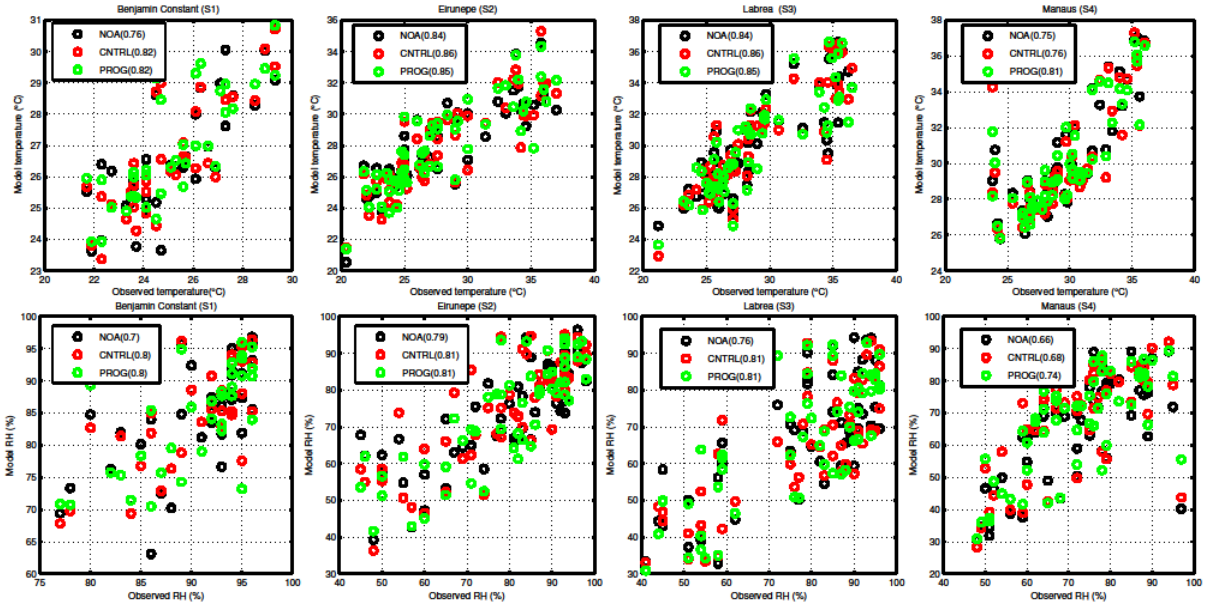

Page 18889, Line 15: Did you check how the distribution of aerosol other than BBA observed during SAMBBA compared with the climatology used in the MetUM model? If the observed distribution is significantly different from the climatology then it may affect the calculation of aerosol optical properties and your conclusions about aerosol-meteorology interaction.

Non-BBA aerosols make such a small contribution to the AODs over the SAMBBA region (6 to 16%) that any deviations of those species from their climatologies will have had a negligible impact on our results.

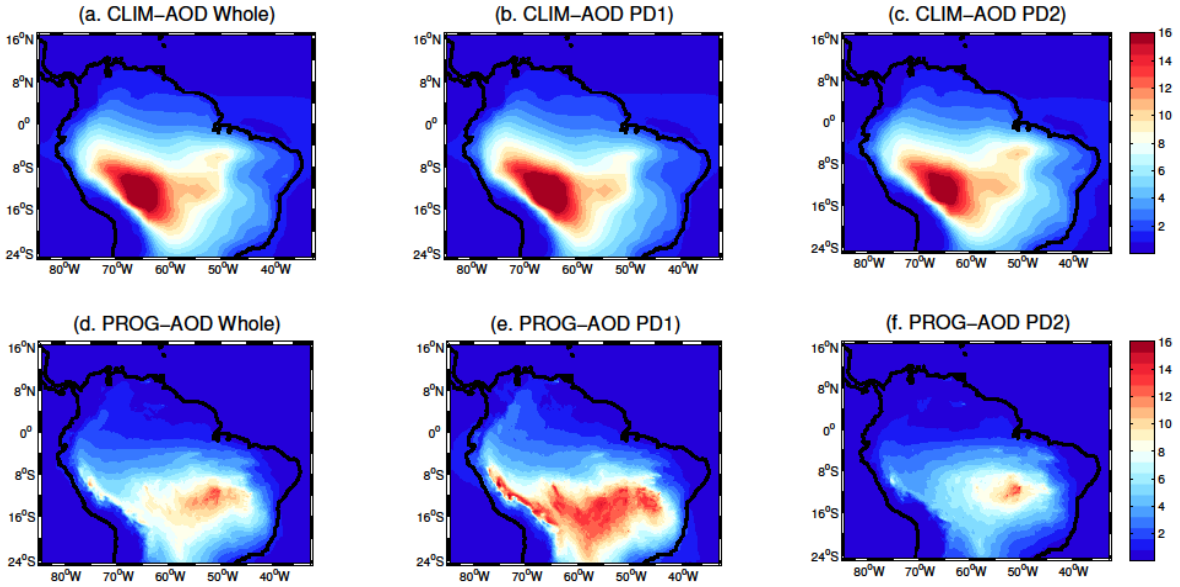

Modelled ratio of BBA AOD to AOD from other species(sulphate+mineral dust+sea salt+soot+fossil fuel). PD1 is period 1, PD2 is period 2, Whole is for whole period. Top row shows CLIM and lower row PROG.

Page 18891, Line 9-13: Can you give a reference for this statement?

This statement is drawn from the Figure 2. We have individually analysed the other species such as sea salt, mineral dust and fossil fuels: these species contribution is very small when compared to large BBA contribution over the Amazonia region. Figure 2 now includes contours of BBA AOD, which show how BBA completely dominates the AODs.

Page 18892, Line 18892: Both MODIS and PROG AOD show large reduction in AOD from

PD1 to PD2 (Fig. 2). Given this, how did you find that effects of BBA were similar during both the periods of SAMBBA?

We mean to say that the effects of BBA qualitatively are similar but quantitatively vary. Our study found that, an increase in impact with increase in aerosols. For clarity, we have changed "During both periods of SAMBBA (PD1 and PD2) *pattern of* **impacts of BBA were found to be similar".**

Page 18892, Lines 18-19: Why are the radiative effects larger on day 2?

This is the case for CLIM and PROG so it cannot simply be from the change in AOD from day 1 to day 2. This is also the case for clear-sky as well as whole-sky, so is not simply due to the different changes in the cloud field between runs. The clear-sky radiative budget is a function of both surface temperature and the temperature and moisture profile of the column, we know these evolve in response to changes in the BBA (Figure 5 and the water vapour budget analysis, which reveals that overall impacts the atmosphere are drying in this study). These must combine to give larger radiative effects on day 2. However, we need to investigate these effects on medium, seasonal and climate scale. We will be investigating these impacts in the future SAMBBA studies.

Page 18892, Line 28: Why do you differ from Ten Hoeve et al.?

Ten Hoever et al. (2012) found BB decreased the net top of the atmosphere solar+IR irradiance modestly, but with large diurnal variation. Their study has both direct, semi direct and indirect aerosols impacts. Ten Hoeve et al. (2012) compared satellite-derived with modeled curves of aerosol optical depth (AOD) versus cloud optical depth (COD) and found that while biomass burning aerosol particles increase CODs with increasing AOD below ~0.2 due to stronger indirect effects than the cloud absorption effects (CAEs) plus semidirect effects (SDEs), BB aerosol particles decrease CODs at higher AODs due to stronger combined CAEs and SDEs than indirect effects. These results suggest that in regions of high BB emissions, BB particles should reduce COD, increasing solar transmission to the surface, warming the surface in a positive feedback. In our study, we have only direct radiative effects and BB aerosol reflect more shortwave radiation back to space. This would imply a cooling of the earth-atmosphere system in our study.

We have added

"**does not agree with results from Ten Hoeve et al. (2012) which showed a positive**

change for higher AODs *and included direct, semi direct and indirect aerosols impacts*

(i.e. Earth–atmosphere warming), *"*

to the paper text.

Page 18894, Lines 16-17: I don't see any red colors above PBL in Fig. 6a. I assume you want to say that green colors in Fig. 6a above PBL represent positive values but it is hard to understand from the color-bar whether these green colors correspond to positive or negative values. I suggest using blue colors for negative values and red colors for positive values. Could you also explain the large cooling seen at 300-400 hPa?

Page 18894, Lines 26-28: Why do you see a warming at 15 km?

We thank reviewer suggestion for changing the color bar. We have changed the color bar in the revised MS. The cooling between 300-400hPa and warming between 200-100hPa effects are addressed in the MS pages 18895-18896 Lines 23-3 and our results supports with others findings.

Page 18894, Lines 20-21: As previously mentioned, please check the statistical significance of these results.

"Differences in BL height in Figure 6b are not statistically significant but physically consistent with flux changes" , **and this is now stated in the text. However, we know that the decreased surface sensible heat flux in the runs with aerosol will lead to reduced entrainment and a shallower BL in the model, and the modelled change in BL height is consistent with this.**

Page 18911, Figure 3: I would suggest using different y-axis scales for different panels. For instance, it is hard to see variations for La Paz. Medellin does not add any value to the model evaluation and thus can be removed.

We thank the reviewer for suggesting the different y-axis scales for different panels. We have adjusted the figure in the revised MS. The variability of AODs at La Paz and Medellin can now be seen more clearly. We still include the Medellin station, as we think it is important to use all available AERONET data and including this plot does not take any additional space in the paper.

Page 18915, Figure 7: Can you use a different color scale to show some variability in ice and liquid cloud water differences? Right now, it looks like that only three values are possible.

As suggested by reviewer, we have used different colour-scale for the figure7. Please see the revised MS.

Page 18916, Figure 8: It is not clear whether white contour represent positive or negative values?

We have re-plotted this figure with negative contour values in dashed lines and positive contours in solid lines. Please find the revised MS.

Minor comments:

Page 18887, Line 4: Change "The weakened in the Hadley circulation causing" to "weakening of the Hadley circulation caused".

We thank reviewer for the suggestion. We have changed this sentence in the revised MS as follows below.

"*This resulted in a weakening of the Hadley circulation, causing small reductions in global precipitation but with larger reductions near the equator***."**

Page 18887, Line 9: Change Paolo to Paulo.

We thank reviewer for typo. We have included this in the revised MS.

Page 18887, Line 14: Add "direct" before "impact of".

We have not included "direct" here because, the SAMBBA projects aims to assess the direct as well as indirect impacts of Amazonian biomass burning aerosols on the regional and global radiation budget. Although this study presents direct impacts but we will be presenting indirect impacts as well in future.

Page 18889, Line 2: Can you please mention the source of chemical initial and boundary conditions?

This is now added to the paper text, *"Meteorological boundary conditions for all runs (3 hourly) are provided by the global operational NWP model (global GA3.1 configuration of the UK at N512 (25 km); Walters et al., 2011). In the PROG, the BBA is free-running for two days, with spin-up of BBA from the beginning of August."*

Page 18894, Line 5: Remove one "surface".
We have removed as suggested.

Manuscript prepared for Atmos. Chem. Phys. Discuss.
with version 2014/09/16 7.15 Copernicus papers of the LaTeX class copernicus.cls.
Date: 15 October 2015

Impacts of Amazonia biomass burning aerosols assessed from short-range weather forecasts

S. R. Kolusu[1], J. H. Marsham[1,2], J. Mulcahy[3], B. Johnson[3], C. Dunning[3], M. Bush[3], and D. V. Spracklen[1]

[1]Institute for Climate and Atmospheric Science, water@leeds, School of Earth and Environment, Leeds, LS2 9JT, UK
[2]National Centre for Atmospheric Science, Leeds, UK
[3]Met Office, FitzRoy Road, Exeter, EX1 3PB, UK

Correspondence to: S. R. Kolusu (s.kolusu@leeds.ac.uk)

Abstract

The direct radiative impacts of Biomass Burning Aerosols (BBA) on meteorology are investigated using short-range forecasts from the Met Office Unified Model (MetUM) over South America during the South American Biomass Burning Analysis (SAMBBA). The impacts are evaluated using a set of three simulations: (i) no aerosols, (ii) with monthly mean aerosol climatologies and (iii) with prognostic aerosols modelled using the Coupled Large-scale Aerosol Simulator for Studies in Climate (CLASSIC) scheme. Comparison with observations show that the prognostic CLASSIC scheme provides the best representation of BBA. The impacts of BBA are quantified over central and southern Amazonia from the first and second day of two day forecasts during 14 September–03 October 2012. On average, during the first day of the forecast, including prognostic BBA reduces the clear-sky net radiation at the surface by $15 \pm 1\,\mathrm{W\,m^{-2}}$, and reduces net TOA radiation by $8 \pm 1\,\mathrm{W\,m^{-2}}$, with a direct atmospheric warming of $7 \pm 1\,\mathrm{W\,m^{-2}}$. BBA-induced reductions in all-sky radiation are smaller in magnitude: $9.0 \pm 1\,\mathrm{W\,m^{-2}}$ at the surface and $4.0 \pm 1\,\mathrm{W\,m^{-2}}$ at TOA. In this modelling study the BBA therefore exert an overall cooling influence on the Earth–atmosphere system, although some levels of the atmosphere are directly warmed by the absorption of solar radiation. Due to the reduction of net radiative flux at the surface the mean 2 m air temperature is reduced by around $0.1 \pm 0.02\,^{\circ}\mathrm{C}$. The BBA also cools the boundary layer (BL) but warms air above by around $0.2\,^{\circ}\mathrm{C}$ due to the absorption of shortwave radiation. The overall impact is to reduce the BL depth by around 19 ± 8 m. These differences in heating lead to a more anticyclonic circulation at 700 hPa, with winds changing by around $0.6\,\mathrm{m\,s^{-1}}$. Inclusion of climatological or prognostic BBA in the MetUM makes a small but significant improvement in forecasts of temperature and relative humidity, but effects were small compared with model error and differences between effects from climatological and prognostic BBA were not significant. Locally, on a 150 km scale, changes in precipitation reach around $4\,\mathrm{mm\,day^{-1}}$ due to changes in the location of convection. Over Amazonia, including BBA in the simulation led to fewer rain events that were more intense. This change may be linked to the BBA changing the vertical profile of stability in the lower atmosphere. The lo-

calised changes in rainfall tend to average out to give a 5 % (0.06 mm day^{-1}) decrease in total precipitation over the Amazonian region (except on day 2 with prognostic BBA). The change in water budget from BBA is, however, dominated by decreased evapotranspiration from the reduced net surface fluxes (0.2 to 0.3 mm day^{-1}), since this term is larger than the corresponding changes in precipitation and water vapour convergence.

1 Introduction

Landscape fires and open biomass burning emit large quantities of trace gases and aerosol to the atmosphere, altering atmospheric composition and impacting weather and climate (Bowman et al., 2009). They are the largest source of carbonaceous aerosols to the atmosphere, contributing 65 % of global total organic carbon (OC) emissions and 25 % of global black carbon (BC) emissions (Lamarque et al., 2010). Moreover, biomass burning contributes to various air pollutants that adversely affect human health (Marlier et al., 2013). Biomass burning aerosols (BBA) can significantly alter the energy balance of the atmosphere and the Earth's surface by directly absorbing and scattering solar radiation (Reid et al., 2005), and indirectly by changing the cloud properties, thus modulating the hydrological cycle (Ramanathan et al., 2001; Andreae and Rosenfeld, 2008). As a result, BBA affects sensible and latent heat fluxes in the lower atmosphere altering the temperature of the Earth's surface (Yu et al., 2002; Ichoku et al., 2003). The direct and indirect effects of BBA cause changes in the regional weather and climate via changes in the stability of the atmosphere, height of the boundary layer (BL), regional atmospheric circulation, cloud formation and precipitation (Kaufman and Koren, 2006; Rosenfeld et al., 2008). Despite such impacts on regional weather, most operational weather forecasts only include a climatological treatment of BBA. Here we explore the impact of prognostic BBA on short-term weather forecasts over Amazonia.

The majority of fires worldwide occur in the tropical countries (Crutzen and Andreae, 1990; van der Werf et al., 2010) and the tropics play a particularly pivotal role in tropospheric chemistry (Crutzen and Zimmermann, 1991). Landscape fires occur due to both

natural and anthropogenic activities, such as forest fires, agricultural crop residue burning and deliberate burning of savannah grasslands, and deforestation for agricultural purposes. South America accounts for an estimated 15 % of global fire emissions of carbon from landscape fires and open biomass burning (van der Werf et al., 2010), with regional hotspots of fire activity around the edges of Amazonia. The Amazon region experiences a large number of fires each dry season (August–October). Emissions of BBA from fires greatly increase regional aerosol concentrations (Martin et al., 2010), with dry season AOD of up to 4 observed at 550 nm using AERONET sun photometers (Artaxo et al., 2013). Such large concentrations of BBA with large AOD values may have substantial impacts on the regional radiative balance. Procopio et al. (2004) used observations during the dry season to estimate that Amazonian BBA caused a clear-sky radiative effect of -5 to $-12\,\mathrm{W\,m^{-2}}$ at top-of-atmosphere (TOA) and -21 to $-74\,\mathrm{W\,m^{-2}}$ at the surface. Furthermore, Sena et al. (2013) used a combination of MODIS and CERES data to estimate daily direct TOA radiative effects, which reached $-30\,\mathrm{W\,m^{-2}}$ locally. Rosário et al. (2013) used a regional model to estimate a surface radiative effect of $-55\,\mathrm{W\,m^{-2}}$. Such changes in fluxes must affect Amazonian weather and a better understanding of this has potential benefits for improving weather and climate prediction.

Modelling studies have explored the impact of BBA on regional weather and climate. Zhang et al. (2008) studied the direct effect of BBA using the regional climate model RegCM3 and found that BBA can weaken regional circulation, cloudiness and perturb land–atmosphere interactions. Zhang et al. (2009) showed that BBA can impact the monsoon circulation weakening the South American monsoon circulation by increasing atmospheric stability. Using WRF-Chem model over South America, Wu et al. (2011) showed that BBA suppressed the diurnal amplitude of convection by about 11 %, decreasing clouds (consistent with Cook and Highwood, 2004) and precipitation in the afternoon but increasing them at night. Using the Community Atmosphere Model version 5 (CAM5), Tosca et al. (2013) found that BBA increased global mean AODs by 10 %, increased tropospheric heating and decreased global surface temperature by $0.13 \pm 0.01\,^{\circ}\mathrm{C}$. This resulted in a weakening of the

Hadley circulation, causing small reductions in global precipitation but with larger reductions near the equator.

The South American Biomass Burning Analysis (SAMBBA) was an international project involving ground-based and aircraft observations led by the UK Met Office, the National Institute for Space Research (INPE) Brazil, a consortium of 7 UK universities and the University of Sao Paulo. The observational flight campaign was conducted from 14 September to 03 October 2012 across Amazonia. SAMBBA aims to assess the impact of Amazonian BBA on the regional and global radiation budget through the direct, semi-direct and indirect effects, on atmospheric dynamics and the hydrological cycle, on numerical weather prediction (NWP) forecasts, on climate, and on air quality. In this study we focus on the objective of quantifying the impact of BBA on weather.

Most operational global weather forecast models include a simplified aerosol representation in the form of climatologies. Mulcahy et al. (2014) found that including a more advanced treatment of aerosols and their radiation-cloud interactions improved NWP model biases. SAMBBA provides an ideal opportunity to evaluate the impact of BBA on the meteorology of Amazonia as well as to evaluate the impact of including prognostic BBA coupled to radiation on the forecast model skill. In this study, we present the direct radiative impacts of BBA on short-range weather forecasts using a limited area version of the Met office Unified Model (MetUM). Cloud-aerosol interactions will be considered in future studies using the MetUM coupled with the more advanced aerosol microphysical model, United Kingdom Chemistry and Aerosol (UKCA). The specific research questions addressed in this study are, (1) what are the impacts of BBA on the mean meteorological state during the SAMBBA period, (2) what are the mechanisms for these impacts and (3) can an improvement in forecast model skill be obtained through use of a fully online BBA model instead of a climatology? To our knowledge, this is the first study which presents the regional scale interactions and feedbacks using prognostic CLASSIC BBA scheme over South America. The paper is organized as follows; Data, model and methods are presented in Sect. 2. Section 3 presents results and discussion. Finally, summary and conclusions are presented in Sect. 4.

2 Model and data

2.1 Model

The MetUM (Davies et al., 2005) is used on a wide range of spatial and temporal scales from high-resolution short-range numerical weather prediction (NWP) to multi-decadal and centennial simulations in an earth system model configuration (Collins et al., 2011). In this study a limited area model (LAM) configuration of the MetUM is set up over Brazil (Fig. 1) with a horizontal grid spacing of 0.1 ° latitude/longitude (around 12 km) and 70 levels in the vertical (model lid at 80 km). Simulations are run covering the SAMBBA campaign period (14 September to 03 October 2012). Meteorological boundary conditions for all runs (3 hourly) are provided by the global operational NWP model (global GA3.1 configuration of the UK at N512 (25 km); (Walters et al., 2011)). In the PROG, the BBA is free-running for two days, with spin-up of BBA from the beginning of August. The atmospheric boundary layer is modelled following Brown et al. (2008) while convection is parameterized using the mass flux scheme based on Gregory and Rowntree (1990). Large-scale precipitation uses the single moment scheme based on Wilson and Ballard (1999), while large-scale cloud is parameterized using the scheme of Smith (1990). Cloud amount is diagnosed as a function of relative humidity by assuming the sub-grid humidity distribution follows a symmetric triangular function centred on the grid-box mean. The width of this distribution is reduced near the surface to account for the reduced variability expected with smaller volume grid-boxes on thinner near-surface model levels. The radiation scheme employed is the 2-stream radiation code of Edwards and Slingo (1996) with 6 and 9 bands in the shortwave (SW) and longwave (LW) parts of the spectrum respectively. The simulations are initialised using a continuous 6 hourly cycle of three-dimensional variational data assimilation (3-D-Var) (Lorenc et al., 2000) with a 2 day forecast run daily at 00:00 UTC (20:00 (UTC − 4) local time in Porto Velho, Brazil).

Three model experiments, encompassing different representations of aerosols, were conducted to investigate the impact of BBA (Table 1). Firstly, a simulation without any aerosol representation (hereafter termed as NOA) is conducted. Secondly, a set of simulations

which include monthly mean speciated aerosol climatologies (hereafter termed as CLIM). The climatologies are generated from HadGEM2 climate simulations using the CLASSIC (Coupled Large-scale Aerosol Simulator for studies in Climate) aerosol scheme (Bellouin et al., 2011). Aerosol species represented include sulphate, mineral dust, biomass burning, OC from fossil fuel, BC from fossil fuel, sea salt and nitrate aerosol. Due to the cost associated with running a fully coupled prognostic aerosol scheme operationally at high spatial resolution the global operational NWP configuration of the MetUM currently uses these monthly climatologies for all aerosol species apart from mineral dust. Finally, prognostic BBA is included using the BBA component of CLASSIC (hereafter named as PROG). In PROG aerosol climatologies are still used for all other aerosol species, i.e. other than BBA.

A full description of the CLASSIC BBA scheme is given in Bellouin et al. (2011). In PROG, daily BBA emissions are taken from the Global Fire Assimilation System (GFAS) version 1.1 emission dataset (Kaiser et al., 2012). These include global emission fluxes from open BB such as deforestation and crop residue burning estimated from satellite-based fire radiative power observations. A number of previous modelling studies have increased BBA emissions by up to a factor 5 to improve model agreement with observed AOD (Marlier et al., 2013; Ward et al., 2012; Tosca et al., 2013). Here, GFAS emissions were scaled by a factor of 1.7 to give improved agreement of modelled AOD against AERONET observations. In all simulations including an aerosol representation, the aerosols are coupled to the radiation scheme (which is called hourly) allowing the direct and semi-direct effect of the aerosols to be simulated. The aerosols do not affect assumed cloud droplet concentrations and so there is no representation of aerosol-cloud microphysical interactions, except for wash-out of BBA by rain in PROG.

2.2 Observational data and Methods

MODIS (Moderate Resolution Imaging Spectroradiometer) Terra level 3 (King et al., 2003) satellite-retrieved daily AOD at 550 nm, with an uncertainty of ± 0.05 over land, ± 0.03 over ocean (Ichoku et al., 2005) and a horizontal resolution of 1° latitude/longitude are used to evaluate simulated AOD. In addition, we use ground-based retrievals of AOD (level 2) at

550 nm from eight AERONET stations in the Amazonia region (Holben et al., 1998). ERA-Interim 6 hourly winds and geopotential height at 850 hPa obtained from the European Centre for Medium-Range Weather Forecasting (ECMWF) with a spatial resolution of 1.5° latitude/longitude (Simmons et al., 2007) have been used to analyse meteorological conditions during the campaign period. For comparison with model simulations we use near-surface temperature and relative humidity observations from different locations over the Amazon region provided by University of Sao Paulo (locations in Fig. 1; data are six-hourly except for Benjamen Constant, which are 12 hourly) and radiosonde data (12 hourly). The impacts of BBA ($\Delta^{\mathrm{BBA}}_{\mathrm{NOA}}$) as a function of forecast lead time t can be defined as a difference $\Delta f(t) = f_{\mathrm{BBA}}(t) - f_{\mathrm{NOA}}(t)$ where, f_{NOA} is any meteorological variable in NOA simulation and f_{BBA} is the same meteorological variable from BBA simulations. In this study, we use the diurnal mean from $t = 0$ to $t + 24$ h, unless otherwise stated. Impacts of other aerosols contributions are small in the Amazonia region during the SAMBBA period.

We have calculated the significant values using the Standard Error (SE) using the following method.The autocorrelation has been accounted for in the time series of each pixel.

$$SE = \frac{SD}{\sqrt{N}} k \tag{1}$$

where “SD” is the standard deviation and “N” is the number of points (i.e how many times contribute to each pixel in the model domain). “k” is the autocorrelation correction factor. This is based on the (Bence , 1995).

$$k = \sqrt{\frac{(1+p)}{(1-p)}} \tag{2}$$

where “p” is the autocorrelation function. “p” is calculated using the Prais-Winsten estimation.

3 Results and discussion

3.1 Meteorological conditions and aerosol distributions during SAMBBA

ERA-Interim analyses and aerosol loadings from the UM are presented in Fig. 2. The data are shown for two distinct periods during the SAMBBA campaign: Period 1 (PD1) from 14–22 September and Period 2 (PD2) from 22 September–03 October 2012. In 2012 there was a transition from the end of the dry season into the wet season around the 22 September (Brito et al., 2014). Periods 1 and 2 therefore had different synoptic conditions and aerosols loadings. Therefore, we analyse results from these two periods separately as well as considering averages from the whole period. Figure 2a–c shows low-level inflow for each period of air into South America from the east, which turns southwards along the edge of Andes. This inflow is stronger in the second period. Detailed synoptic weather conditions for all the SAMBBA flights are presented in the SAMBBA campaign summary booklet (Darbyshire and Johnson, 2013).

Figure 2 presents the total AOD (550 nm) from MODIS observations, CLIM and PROG simulations for the whole SAMBBA period, as well as PD1 and PD2. AODs were notably higher during PD1 in both the MODIS data and PROG. This difference is due to BBA, since other species such as sea salt, sulphate, mineral dust make very small contributions over South America during the dry season and the AOD maximum is dominated by BBA. Mean AOD's from MODIS show a significant year-to-year variations in AODs and that 2012 is a below average year (not shown). MODIS has a high aerosol loading in the east ($\sim$ 60–50° W) with lower AODs in the west. The CLIM simulation shows large positive bias compared with MODIS particularly in the west of Brazil (around 65° W). As CLIM uses monthly mean aerosol fields it can not capture the reduction in AOD observed in PD2. The PROG simulation is better able to capture the temporal and spatial variability of AOD for all periods. It captures the decrease in AODs in PD2 and the location of the maximum AOD to within 5°. Both PROG and CLIM, have too low AOD north of 8° S, with both models giving too weak local maxima around 8° S.

Figure 3 compares a timeseries of the instantaneous observed AOD from AERONET with 6 hourly instantaneous values from the model simulations. PROG is able to simulate the day to day variations in AOD at the different AERONET sites, unlike CLIM where any variation in AOD is due solely to changes in the relative humidity. This is demonstrated by positive correlations between AERONET and PROG at all sites except for Medellin (where there are very few data and a single AOD peak is missed giving a correlation of -0.1). The mean correlation of AOD between AERONET and PROG is 0.4 and is -0.1 for CLIM. However, both PROG and CLIM fail to simulate very high AOD observed at Alta Floresta, Rio Branco and Santa Cruz (Fig. 1), although some discrepancy may arise from comparing a grid-box mean with a point observation from AERONET. Our analysis demonstrates that PROG better captures the observed spatial and temporal variability in BBA over the SAMBBA period.

3.2 Radiative impacts of BBA

During both periods of SAMBBA (PD1 and PD2) pattern of impacts of BBA were found to be similar and we therefore focus on the whole SAMBBA period in the remainder of our analysis. Differences in the simulated net radiation fields are calculated relative to NOA for clear-sky conditions at the surface (Fig. 4a and d) and at the top-of-atmosphere (TOA) (Fig. 4b and e). The net atmospheric divergence (ATM) is calculated as the net radiation at TOA minus net radiation at the surface, giving the change in absorption of radiation in the atmosphere. A summary of the radiative impacts is shown in Table 2, together with their standard deviations, with standard errors in brackets (the standard error will be an under-estimate of uncertainty as the data points contributing to the mean are not independent). Values are calculated over the region of box A (shown in Fig. 1) for the whole period for both day 1 and day 2 of the forecast. BBA scatters and absorbs solar radiation reducing the net surface radiation in CLIM and PROG compared with NOA (see Fig. 4a and d) i.e. the BBA cools the surface. The radiative impacts are larger in magnitude in the CLIM simulation than in the PROG simulation (see Table 2) due to its larger AODs, particularly in western Brazil. In PROG and CLIM the radiative effects are larger on day 2 than the day 1.

In this model, BBA decreases net clear-sky TOA radiation over Amazonia (Fig. 4b and e). Biomass burning aerosol species in the CLASSIC scheme have a relatively high single scattering albedo (dry value of 0.91 at 550 nm, increasing to 0.95 at 80 % relative humidity) and much of the Amazonian region considered in this study contains forest or vegetated surface with relatively low surface albedos. In clear-sky, the impact on net radiation at TOA ranges from 0 to $-25\,\mathrm{W\,m^{-2}}$ for CLIM and 0 to $-15\,\mathrm{W\,m^{-2}}$ for PROG (again with larger impacts found in day 2 in PROG as well as in CLIM, Table 2). The negative change in net TOA radiation (consistent with Haywood and Boucher, 2000; Procopio et al., 2004; Sena et al., 2013) does not agree with results from Ten Hoeve et al. (2012) which showed a positive change for higher AODs(i.e. Earth–atmosphere warming) and included direct, semi direct and indirect aerosols impacts , and the magnitude of the change in surface radiation is consistent with other studies (Procopio et al., 2004; Kaufman and Koren, 2006; Rosenfeld et al., 2008; Sena et al., 2013). The increase in radiative absorption across the atmosphere (ATM) is between 10 and $20\,\mathrm{W\,m^{-2}}$ (slightly greater in CLIM than PROG due to greater AODs) (Fig. 4c and f). The radiative absorption range by aerosols in the atmosphere found for the whole period is in good agreement with the value of $18.7\,\mathrm{W\,m^{-2}}$ found in a case study from the same period using the WRF-Chem model (which includes prognostic BBA with both direct and indirect effects from (Archer-Nicholls et al., 2015).

More subtle impacts on model cloud fields are found in PROG and CLIM on horizontal scales of one degree and a systematic decrease in high and medium cloud fraction of around 0.1 is found in areas of highest AODs (cloud changes are described later in Sect. 3.3). This may be a result of BBA stabilising the atmosphere, as discussed in Sects. 1 and 3.3. Changes in all-sky net radiation, which include the impacts of changes in the cloud fields resulting from BBA's direct effects, are lower in magnitude by around a factor of two compared with clear-sky values (Table 2), but the overall patterns are similar (not shown), i.e. the reduced cloud in PROG and CLIM compared with NOA decreases the magnitude of the surface and TOA cooling induced by the BBA.

3.3 Impacts of BBA on atmospheric thermodynamics

Over the whole SAMBBA period, the decrease in net surface radiation from BBA decreases the mean 2 m air temperatures by up to 1.4 °C, but with local increases of up to about 0.5 °C due to changes in cloud (Fig. 5). In PROG, the mean impact over Box A is a 0.1 °C decrease on day 1, reaching 0.2 °C decrease on day 2 (Table 2; effect is 0.03 °C larger in CLIM). The largest changes are found, as expected, close to regions of maximum BBA. The differences are largely restricted to the land, where air temperatures respond to the modelled surface energy balance. Tosca et al. (2010) showed that BBA can affect SSTs around Indonesia, but in all simulations here the SSTs are prescribed from reanalysis. Over land, the BBA cools the surface skin temperature by approximately 0.2 °C on day 1 and 0.3 °C on day 2. Over Box A 10 m wind-speeds are reduced (Table 2), likely due to decreased surface sensible heat fluxes reducing downward mixing of momentum to the surface.

The impacts of BBA on atmospheric radiative and surface heating rates affects the thermodynamic structure of the atmosphere far above the surface. Figure 6a shows potential temperature cross sections averaged over the 10 to 13° S latitude belt, chosen as it is the region where surface impacts of BBA are largest in Figs. 4 and 5. Figure 6a and b are plotted for 18:00 UTC (14:00 local time) in order to show a well developed afternoon BL, with BL depth shown for NOA (white line) and PROG (red line). BBA mass concentrations (contoured) are well mixed within the BL and extend higher in the east where the BL is deeper (around 400 hPa, compared with 500 hPa in the west). Figure 6a shows that BBA cools the lower atmosphere over land (blue colours in Fig. 6a), consistent with the reduced net surface radiation. This cooling is deeper in the east where the BL is deeper (reaching around 700 hPa). BBA warms the atmosphere above this (red colours in Fig. 6a) with this warming centered around the top of the BL, or just above it. This warming is consistent with the direct radiative effects of the BBA, extending higher in the east where the BBA extends higher. The reduced net surface radiation from BBA reduces surface fluxes and this, combined with the increased atmospheric heating from BBA, reduces entrainment into the BL, and so BL depth reduces by up to 150 m (Fig. 6b) with a daily mean impact of 19 m over

Box A (Table 2). Differences in BL height in Figure 6b are not statistically significant but physically consistent with flux changes.

Figure 6 shows that the effects of BBA on temperatures above the surface layer are between -0.2 and $+0.2\,^{\circ}\mathrm{C}$ when averaged over the entire SAMBBA period ($\sim \pm 0.4\,^{\circ}\mathrm{C}$ in the first sub-period, with similar patterns, not shown). The effect of the BBA on temperature extend well above the BBA, with effects between 100 to 400 hPa as large as those lower in the atmosphere. Overall, there is a weak cooling at the surface and above the aerosol layer at 500 hPa, and warming at 150 hPa (corresponding to approximately 15 km altitude). These changes are consistent with Chen et al. (2014) who simulated radiative effects during a wild fire event over the United States using WRF-Chem model. These are also consistent with changes in vertical motion induced by the BBA, as discussed below.

Cross-sections of relative humidity (RH), ice cloud water (QCF), liquid cloud water (QCL) are presented in Fig. 7 at 18:00 UTC, in a similar manner to Fig. 6a for potential temperature. Differences in the RH profiles are consistent with changes in the potential temperature profile within the BL. BBA tends to decrease RH above the BL (Fig. 7a), consistent with the warming induced there (Fig. 6a), although differences in the patterns shown in Figs. 6a and 7 show that changes in water vapour mixing ratio (WVMR) are also important for RH. Consistent with the decrease in RH from BBA above the BL, BBA decreases both QCF and QCL (Fig. 7b, and c), i.e BBA suppresses middle and high level clouds, consistent with aerosol semi-direct effects from other studies (Jacobson, 2002; Korontzi et al., 2004; Wu et al., 2011; Chen et al., 2014).

Figure 8a shows changes in geopotential and horizontal and vertical winds for the same cross-section as Fig. 6a. The surface cooling with heating above, induced by the BBA, which has a vertical extent that depends on the BL depth and height of the BBA, and an intensity that depends on the BBA loading, induces a weak surface high pressure around 50° W and a weak low pressure at 65° W (Fig. 8a). Low-level wind changes are consistent with this, but only reach $0.5\,\mathrm{m\,s^{-1}}$. The effects are stronger at 700 hPa, where the horizontal gradient in BL depth and BBA heating gives a low pressure relative to NOA at around 50° W and a relative high pressure at 65° W. This gives a weak anti cyclonic circulation

at this level in the runs with BBA compared with NOA (Fig. 8b), with differences in winds reaching 0.6 m s^{-1}.

Changes in winds above 400 hPa are again consistent with the changes in geopotential there, and are larger than below, due to the strong winds at this level in the atmosphere. Figure 8a shows that BBA generates ascent and so cooling centered at around 350 hPa and 65° W and descent above, consistent with the cooling and warming shown at these levels in Fig. 6a. Small changes in vertical winds (Fig. 8a white lines) cause relatively large changes in temperature at these heights in the atmosphere, which are very stable. The fact that the temperature changes at these levels are consistent with vertical motion induced by BBA, suggests an upper level wave response to the direct effects and heating from the BBA below. Similar patterns are found in the CLIM but the impacts are larger where the AOD is higher.

3.4 Evaluation of BBA impacts on the short-range forecasts

The majority of regional and global operational NWP models currently use a climatological representation of aerosols. Here the impact of BBA on the NWP forecast skill is evaluated in order to ascertain if a more advanced treatment of aerosols leads to an improvement in model predictions. Figure 9 shows the mean bias and root mean square (RMS) error in modelled 2 m temperatures as a function of forecast lead time at the 4 sites shown in Fig. 1 averaged over the whole period. The inclusion of aerosols tends to improve the surface temperatures biases in forecasts , but improvements are small compared with mean bias and RMS error. Mean correlations between observations (S1 to S4 locations in Fig. 1) and modelled values are significant and are always higher for PROG or CLIM than NOA (e.g. for temperature (relative humidity), 0.83 (0.79) for PROG and 0.82 (0.77) for CLIM compared with 0.79 (0.72) for NOA). This difference between PROG or CLIM and NOA is significant at the 85 % level (Hoerger, 2013) and shows that including BBA leads to a small improvement in 2 m temperature. Differences between CLIM and PROG are not significant and it is clear from Fig. 9 that including a fully prognostic BBA scheme does not lead to a significant improvement in skill relative to CLIM, although more observations from the west of the

domain where aerosol fields of PROG and CLIM show greater differences, might reveal more benefits of PROG compared with CLIM.

Figure 10 presents the mean bias in simulated temperature and relative humidity profiles at Porto Velho and Boa Vista for the entire SAMBBA period compared to radiosondes at 00:00 and 12:00 UTC. Mean temperature errors are less than 1 °C above 850 hPa, but reach 5 °C at the surface in Porto Velho. Relative humidity errors reach ±20 % and are again largest closest to the surface. These large biases at 00:00 UTC in the model near the surface are due to the model failing to accurately capture the nocturnal stable layer, a common problem in regional NWP models. For temperature and humidity, differences between the aerosol simuations are generally small apart from at Boa Vista where PROG leads to an increase in relative humidity above 850 hPa. The model biases in temperature will affect vertical mixing of aerosol, but we do not anticipate that they substantially affect modelled sensitivities to BBA.

3.5 Impacts of BBA on precipitation and the water budget

Although the simulations conducted in this study do not couple the BBA with cloud microphysical processes, the BBA can alter precipitation as direct radiative effects have an impact on clouds and convection. Figure 11a shows the mean precipitation rate averaged over the whole campaign for the NOA simulation. There are large local differences in mean rainfall between the three simulations (NOA, PROG, CLIM) (Fig. 11b and c), mainly due to changes in the location of precipitation events. When smoothed over a 150 km grid these changes are still around 4 $\mathrm{mm\,day^{-1}}$, although the change in the regional mean is small: for Box A (Fig. 11a), BBA in PROG or CLIM reduces rain by around 0.055 $\mathrm{mm\,day^{-1}}$ compared with NOA (mean rainfall is 1.2 $\mathrm{mm\,day^{-1}}$). Precipitation reductions of $\sim$ 5 % found in this study are therefore slightly greater than the Tosca et al. (2013) study which shows a (2 %) decrease over Amazonia.

Changes in the pdf of rainfall over Box A are shown in Fig. 11d and e, with absolute changes in the pdf shown in grey and fractional changes in blue. For both PROG and CLIM, BBA tends to increase the frequency of both no rainfall and the highest rainfall rates, while

decreasing moderate rainfall rates. A Kolmogorov–Smirnov test conducted for the samples showed that the results are statistically significant at 98 % confidence level. This effect on rain-rates may be linked to BBA increasing stability in the lower atmosphere, due to reduced net surface flux and increased radiative warming of the atmosphere.

To further explore the mechanisms for simulated changes in rainfall we calculated the water budget over Box A for all model simulations on day 1 and day 2. BBA reduces the net radiation, this causes a decrease in surface evapotranspiration (0.2 and 0.3 $\mathrm{mm\,day^{-1}}$ in PROG and CLIM, a 5 and 6 % decrease respectively, Table 2). The radiative heating from the BBA enhances the stability of the atmosphere generally reduces precipitation by 0.05 to 0.12 $\mathrm{mm\,day^{-1}}$, except in day 2 of PROG which shows a small (0.02 $\mathrm{mm\,day^{-1}}$) increase. The change in water vapour convergence into box A is unclear with small increases and decreases in PROG and CLIM for days 1 and 2 (-0.02 to $+0.1$ $\mathrm{mm\,day^{-1}}$). The overall consequence is that the change in water budget of box A from BBA is dominated by the reduction in surface evapotranspiration resulting from the decreased net surface radiation. Therefore, the overall net effect of BBA is a drying of the atmosphere in the Amazonian region, largely due to reduced latent heat fluxes. The drying of the atmosphere due to BBA will be further investigated in future studies using the United Kingdom Chemistry and Aerosol (UKCA) model, including indirect radiative effects.

4 Summary and conclusions

A limited area version of the Met Office Unified Model (MetUM) is used to investigate direct radiative effects of biomass burning aerosol (BBA) over tropical South America during the end of the dry season (the SAMBBA period of 14 September to 03 October 2012) and impacts on the atmosphere and short-range weather forecasts. Three simulations were conducted with different aerosols representations: (i) no aerosols (NOA), (ii) monthly mean climatology BBA (CLIM), (iii) BBA modelled prognostically with the CLASSIC aerosol scheme (PROG). Impacts are quantified from the first 2 days of forecasts initialised from meteorological analyses.

The modelled BBA reduced clear-sky net radiation at the TOA by 8 $W\,m^{-2}$ over the region studied and reduced clear-sky net radiation at the surface by on average of 15 $W\,m^{-2}$, with direct warming of the atmosphere due to absorption of solar radiation of 7 $W\,m^{-2}$. BBA reduced cloud cover and all-sky radiative effects were lower than clear-sky effects: -4 and $-9\,W\,m^{-2}$ for the TOA and surface net radiative effects, respectively. The reduced net surface radiation from BBA cooled the mean 2 m air temperature by on average 0.1 °C. The temperature changes found here are less than the ~ -0.3 °C changes found by Wu et al. (2011) using WRF–Chem model over the South America during the dry period of September 2011. This difference in results is consistent with the higher AODs in the Wu et al. (2011) study. We also expect BBA impacts to be greater in an average year, when compared with 2012, which had lower than average AOD values (i.e. approximate half the size).

The BBA cools the lower BL by around 0.2 °C, but heats the atmosphere above by up to 0.2 °C in the elevated BBA layer that extend to between 600 and 400 hPa. The cooling of the BL is consistent with the BBA reducing surface sensible heat fluxes. This reduces BL growth and results in a decrease in the mean BL depth by around 19 m. The BBA induces a weak (0.2 $m\,s^{-1}$) cyclonic circulation in the lower BL, with a weak anticyclonic circulation above (up to 0.6 $m\,s^{-1}$) due to the horizontal gradients in BBA heating. Effects of BBA are communicated to the upper troposphere due to changes in uplift and subsidence affecting mean upper tropospheric temperatures by up to $+0.2$ °C.

The evaluation against observations shows that the model simulations that included aerosols gave a better representation of near-surface air temperature and relative humidity than models without aerosols (mean correlation of 0.79 and 0.72 in NOA compared to 0.83 and 0.79 in PROG for near surface air temperature and RH respectively with 99 % significant confidence level). However, the improvements were small compared with model error. The difference in results between simulations with a climatological and prognostic representation of aerosols were even smaller and statistically insignificant. Similarly, comparison with radiosondes show negligible differences from including BBA compared with model error. These results suggest that while inclusion of a realistic representation of BBA has impacts

on the model radiation fields, improvements on the mean forecast skill are small at the 2 day forecast lead times analysed in this study. This is most likely due to the strong constraint of the 3-D-VAR data assimilation at short forecast lead times. Indeed impacts on the meteorology on day 2 of the forecast were larger than on day 1 (Table 2) indicating that prognostic BBA might have larger impacts on longer medium to seasonal range weather forecast and on climate simulations. Future studies within SAMBBA will investigate this using individual case studies from the SAMBBA period.

The inclusion of a prognostic BBA scheme gives a superior aerosol forecast compared to an aerosol climatology, but in this study did not improve the mean model skill for temperature and relative humidity significantly over that of the BBA climatology. This reiterates the findings of Mulcahy et al. (2014) that the inclusion of realistic aerosol-radiative interactions are of key importance in operational NWP forecasting systems, but that in many cases a monthly varying speciated aerosol climatology can provide sufficient skill. However, given the highly variable nature of BB emissions the more advanced fully prognostic treatment of BBA is required in order to provide an accurate aerosol prediction capability.

In this study PROG and CLIM BBA tended to reduce mean precipitation by around 5 % ($0.06\,\mathrm{mm\,day^{-1}}$, Table 2), although PROG gave a small increase on day 2 ($0.02\,\mathrm{mm\,day^{-1}}$). It can be speculated that such reductions may lead to more biomass burning over Amazonia (Aragao et al., 2014). However, it should be noted that aerosol-cloud feedbacks on cloud brightness, lifetime and precipitation efficiency, which may alter the sensitivity of precipitation to BBA, were not modelled in this study. The BBA also led to changes in the location of convection, resulting in localised changes in precipitation of around $4\,\mathrm{mm\,day^{-1}}$, when smoothed on a 150 km scale. Furthermore, the BBA decreased the frequency of moderate rain rates, and increased the frequency of both no rain and high rain rates. These changes in the distribution of rainfall intensity may be linked to the stabilisation of the lower atmosphere by BBA through the direct radiative effects.

The water vapour budget analysis over the Amazonian region reveals that by reducing the net surface radiation, the BBA reduces surface latent heat fluxes by $0.2\,\mathrm{mm\,day^{-1}}$. There is a drying of the atmosphere as this reduction in latent heat fluxes is not compensated by the

reduced precipitation (around $-0.06\,\mathrm{mm\,day^{-1}}$), or increased water vapour convergence (-0.02 to $+0.1\,\mathrm{mm\,day^{-1}}$). Such impacts of BBA on the water budget of Amazonia will be investigated in future SAMBBA modelling studies using longer simulations that are more free to evolve away from their initial state.

Acknowledgements. The MODIS data used in this study were produced with the Giovanni online data system, developed and maintained by the National Aeronautics and Space Administration (NASA) GES DISC. We acknowledge the MODIS teams for the data used. We thank Jim Haywood for a careful reading and discussion of the manuscript. We thank the Principal investigators and their staff for establishing and maintaining the 8 AERONET sites used in this investigation. The Facility for Airborne Atmospheric Measurement (FAAM) BAe-146 Atmospheric Research Aircraft is jointly funded by the Met Office and Natural Environment Research Council (NERC) and operated by DirectFlight Ltd. We would like to the dedicated efforts of FAAM, DirectFlight, the National Institute for Space Research (INPE), University of Sao Paulo, and the Brazilian Ministry of Science and Technology in making the SAMBBA measurement campaign possible. We thank to Joel Brito from University of Sao Paulo for providing surface observation over the Amazonia state. The SAMBBA project was funded by the Met Office and NERC with grant number NE/J009822/1. We acknowledge use of the MONSooN system, a collaborative facility supplied under the Joint Weather and Climate Research Programme, which is a strategic partnership between the Met Office and NERC. We thank the three anonymous revieweres for their comments of our manuscript.

References

Andreae, M. and Rosenfeld, D.: Aerosol–cloud–precipitation interactions. Part 1. The nature and sources of cloud-active aerosols, Earth-Sci. Rev., 89, 13–41, 2008.

Aragao, L. E., Poulter, B., Barlow, J. B., Anderson, L. O., Malhi, Y., Saatchi, S., Phillips, O. L., and Gloor, E.: Environmental change and the carbon balance of Amazonian forests, Biol. Rev., 89, 913–931, 2014.

Archer-Nicholls, S., Lowe, D., Schultz, D. M., and McFiggans, G.: Aerosol-radiation-cloud interactions in a regional coupled model: a comparison of the effects of convective parameterisation and resolution, in preparation, 2015.

Artaxo, P., Rizzo, L. V., Brito, J. F., Barbosa, H. M., Arana, A., Sena, E. T., Cirino, G. G., Bastos, W., Martin, S. T., and Andreae, M. O.: Atmospheric aerosols in Amazonia and land use change: from natural biogenic to biomass burning conditions, Faraday Discuss., 165, 203–235, 2013.

Bellouin, N., Rae, J., Jones, A., Johnson, C., Haywood, J., and Boucher, O.: Aerosol forcing in the Climate Model Intercomparison Project (CMIP5) simulations by HadGEM2-ES and the role of ammonium nitrate, J. Geophys. Res.-Atmos., 116, D20206, doi:10.1029/2011JD016074, 2011.

Bence, J. R. (1995). Analysis of short time series: correcting for autocorrelation. Ecology, 628-639.

Bowman, D. M. J. S., Balch, J. K., Artaxo, P., Bond, W. J., Carlson, J. M., Cochrane, M. A., D'Antonio, C. M., DeFries, R. S., Doyle, J. C., Harrison, S. P., Johnston, F. H., Keeley, J. E., Krawchuk, M. A., Kull, C. A., Marston, J. B., Moritz, M. A., Prentice, I. C., Roos, C. I., Scott, A. C., Swetnam, T. W., van der Werf, G. R., and Pyne, S. J.: Fire in the Earth system, Science, 324, 481–484, 2009.

Brito, J., Rizzo, L. V., Morgan, W. T., Coe, H., Johnson, B., Haywood, J., Longo, K., Freitas, S., Andreae, M. O., and Artaxo, P.: Ground-based aerosol characterization during the South American Biomass Burning Analysis (SAMBBA) field experiment, Atmos. Chem. Phys., 14, 12069–12083, doi:10.5194/acp-14-12069-2014, 2014.

Brown, A., Beare, R., Edwards, J., Lock, A., Keogh, S., Milton, S., and Walters, D.: Upgrades to the boundary-layer scheme in the Met Office numerical weather prediction model, Bound.-Lay. Meteorol., 128, 117–132, 2008.

Chen, D., Liu, Z., Schwartz, C. S., Lin, H.-C., Cetola, J. D., Gu, Y., and Xue, L.: The impact of aerosol optical depth assimilation on aerosol forecasts and radiative effects during a wild fire event over the United States, Geosci. Model Dev., 7, 2709–2715, doi:10.5194/gmd-7-2709-2014, 2014.

Collins, W. J., Bellouin, N., Doutriaux-Boucher, M., Gedney, N., Halloran, P., Hinton, T., Hughes, J., Jones, C. D., Joshi, M., Liddicoat, S., Martin, G., O'Connor, F., Rae, J., Senior, C., Sitch, S., Totterdell, I., Wiltshire, A., and Woodward, S.: Development and evaluation of an Earth-System model – HadGEM2, Geosci. Model Dev., 4, 1051–1075, doi:10.5194/gmd-4-1051-2011, 2011.

Cook, J. and Highwood, E.: Climate response to tropospheric absorbing aerosols in an intermediate general-circulation model, Q. J. Roy. Meteor. Soc., 130, 175–191, 2004.

Crutzen, P. J. and Andreae, M. O.: Biomass burning in the tropics: Impact on atmospheric chemistry and biogeochemical cycles, Science, 250, 1669–1678, 1990.

Crutzen, P. J. and Zimmermann, P. H.: The changing photochemistry of the troposphere, Tellus B, 43, 136–151, 1991.

Darbyshire, E. and Johnson, B.: The South American Biomass Burning Analysis (SAMBBA) Field Experiment, September–October 2012, Brazil: Summary of Research Flights, The University of Manchester and the Met Office, available on request from the authors, 1–180, 2013.

Davies, T., Cullen, M., Malcolm, A., Mawson, M., Staniforth, A., White, A., and Wood, N.: A new dynamical core for the Met Office's global and regional modelling of the atmosphere, Q. J. Roy. Meteor. Soc., 131, 1759–1782, 2005.

Edwards, J. and Slingo, A.: Studies with a flexible new radiation code. I: Choosing a configuration for a large-scale model, Q. J. Roy. Meteor. Soc., 122, 689–719, 1996.

Gregory, D. and Rowntree, P.: A mass flux convection scheme with representation of cloud ensemble characteristics and stability-dependent closure, Mon. Weather Rev., 118, 1483–1506, 1990.

Haywood, J. and Boucher, O.: Estimates of the direct and indirect radiative forcing due to tropospheric aerosols: a review, Reviews of Geophysics-Richmond Virginia then Washington, 38, 513–543, 2000.

Hoerger, M.: ZH: an updated version of Steiger's Z and web-based calculator for testing the statistical significance of the difference between dependent correlations, retrieved 1 March 2014, 2013.

Holben, B. N., Eck, T. F., Slutsker, I., Tanré, D., Buis, J. P., Setzer, A., Vermote, E., Reagan, J. A., Kaufman, Y. J., Nakajima, T., Lavenu, F., Jankowiak, I., and Smirnov, A.: AERONET – a federated instrument network and data archive for aerosol characterization, Remote Sens. Environ., 66, 1–16, 1998.

Ichoku, C., Remer, L. A., Kaufman, Y. J., Levy, R., Chu, D. A., Tanré, D., and Holben, B. N.: MODIS observation of aerosols and estimation of aerosol radiative forcing over southern Africa during SAFARI 2000, J. Geophys. Res.-Atmos., 108, 8499, doi:10.1029/2002JD002366, 2003.

Ichoku, C., Remer, L. A., and Eck, T. F.: Quantitative evaluation and intercomparison of morning and afternoon Moderate Resolution Imaging Spectroradiometer (MODIS) aerosol measurements from Terra and Aqua, J. Geophys. Res.-Atmos., 110, D10S03, doi:10.1029/2004JD004987, 2005.

Jacobson, M. Z.: Control of fossil-fuel particulate black carbon and organic matter, possibly the most effective method of slowing global warming, J. Geophys. Res.-Atmos., 107, 4410, doi:10.1029/2001JD001376, 2002.

Kaiser, J. W., Heil, A., Andreae, M. O., Benedetti, A., Chubarova, N., Jones, L., Morcrette, J.-J., Razinger, M., Schultz, M. G., Suttie, M., and van der Werf, G. R.: Biomass burning emissions estimated with a global fire assimilation system based on observed fire radiative power, Biogeosciences, 9, 527–554, doi:10.5194/bg-9-527-2012, 2012.

Kaufman, Y. J. and Koren, I.: Smoke and pollution aerosol effect on cloud cover, Science, 313, 655–658, 2006.

King, M. D., Menzel, W. P., Kaufman, Y. J., Tanré, D., Gao, B.-C., Platnick, S., Ackerman, S. A., Remer, L. A., Pincus, R., and Hubanks, P. A.: Cloud and aerosol properties, precipitable water, and profiles of temperature and water vapor from MODIS, IEEE T. Geosci. Remote, 41, 442–458, 2003.

Korontzi, S., Roy, D. P., Justice, C. O., and Ward, D. E.: Modeling and sensitivity analysis of fire emissions in southern Africa during SAFARI 2000, Remote Sens. Environ., 92, 376–396, 2004.

Lamarque, J.-F., Bond, T. C., Eyring, V., Granier, C., Heil, A., Klimont, Z., Lee, D., Liousse, C., Mieville, A., Owen, B., Schultz, M. G., Shindell, D., Smith, S. J., Stehfest, E., Van Aardenne, J., Cooper, O. R., Kainuma, M., Mahowald, N., McConnell, J. R., Naik, V., Riahi, K., and van Vuuren, D. P.: Historical (1850–2000) gridded anthropogenic and biomass burning emissions of reactive gases and aerosols: methodology and application, Atmos. Chem. Phys., 10, 7017–7039, doi:10.5194/acp-10-7017-2010, 2010.

Lorenc, A. C., Ballard, S. P., Bell, R. S., Ingleby, N. B., Andrews, P. L. F., Barker, D. M., Bray, J. R., Clayton, A. M., Dalby, T., Li, D., Payne, T. J., and Saunders, F. W.: The Met. Office global three-dimensional variational data assimilation scheme, Q. J. Roy. Meteor. Soc., 126, 2991–3012, 2000.

Marlier, M. E., DeFries, R. S., Voulgarakis, A., Kinney, P. L., Randerson, J. T., Shindell, D. T., Chen, Y., and Faluvegi, G.: El Nino and health risks from landscape fire emissions in southeast Asia, Nature climate change, 3, 131–136, 2013.

Martin, S. T., Andreae, M. O., Artaxo, P., Baumgardner, D., Chen, Q., Goldstein, A. H., Guenther, A., Heald, C. L., Mayol-Bracero, O. L., McMurry, P. H., Pauliquevis, T., Pöschl, U., Prather, K. A., Roberts, G. C., Saleska, S. R., Silva-Dias, M. A., Spracklen, D. V., Swietlicki, E., and Trebs, I.: Sources and properties of Amazonian aerosol particles, Rev. Geophys., 48, RG2002, doi:10.1029/2008RG000280, 2010.

Mulcahy, J. P., Walters, D. N., Bellouin, N., and Milton, S. F.: Impacts of increasing the aerosol complexity in the Met Office global numerical weather prediction model, Atmos. Chem. Phys., 14, 4749–4778, doi:10.5194/acp-14-4749-2014, 2014.

Procopio, A., Artaxo, P., Kaufman, Y., Remer, L., Schafer, J., and Holben, B.: Multiyear analysis of Amazonian biomass burning smoke radiative forcing of climate, Geophys. Res. Lett., 31, L03108, doi:10.1029/2003GL018646, 2004.

Ramanathan, V., Crutzen, P., Kiehl, J., and Rosenfeld, D.: Aerosols, climate, and the hydrological cycle, Science, 294, 2119–2124, 2001.

Reid, J. S., Eck, T. F., Christopher, S. A., Koppmann, R., Dubovik, O., Eleuterio, D. P., Holben, B. N., Reid, E. A., and Zhang, J.: A review of biomass burning emissions part III: intensive optical properties of biomass burning particles, Atmos. Chem. Phys., 5, 827–849, doi:10.5194/acp-5-827-2005, 2005.

Rosário, N. E., Longo, K. M., Freitas, S. R., Yamasoe, M. A., and Fonseca, R. M.: Modeling the South American regional smoke plume: aerosol optical depth variability and surface shortwave flux perturbation, Atmos. Chem. Phys., 13, 2923–2938, doi:10.5194/acp-13-2923-2013, 2013.

Rosenfeld, D., Lohmann, U., Raga, G. B., O'Dowd, C. D., Kulmala, M., Fuzzi, S., Reissell, A., and Andreae, M. O.: Flood or drought: how do aerosols affect precipitation?, Science, 321, 1309–1313, 2008.

Sena, E. T., Artaxo, P., and Correia, A. L.: Spatial variability of the direct radiative forcing of biomass burning aerosols and the effects of land use change in Amazonia, Atmos. Chem. Phys., 13, 1261–1275, doi:10.5194/acp-13-1261-2013, 2013.

Simmons, A., Uppala, S., Dee, D., and Kobayashi, S.: ERA-interim: new ECMWF reanalysis products from 1989 onwards, ECMWF Newsletter, 110, 25–35, 2007.

Smith, R.: A scheme for predicting layer clouds and their water content in a general circulation model, Q. J. Roy. Meteor. Soc., 116, 435–460, 1990.

Ten Hoeve, J. E., Jacobson, M. Z., and Remer, L. A.: Comparing results from a physical model with satellite and in situ observations to determine whether biomass burning aerosols over the Amazon brighten or burn off clouds, J. Geophys. Res.-Atmos., 117, D08203, doi:10.1029/2011JD016856, 2012.

Tosca, M. G., Randerson, J. T., Zender, C. S., Flanner, M. G., and Rasch, P. J.: Do biomass burning aerosols intensify drought in equatorial Asia during El Niño?, Atmos. Chem. Phys., 10, 3515–3528, doi:10.5194/acp-10-3515-2010, 2010.

Tosca, M. G., Randerson, J. T., and Zender, C. S.: Global impact of smoke aerosols from landscape fires on climate and the Hadley circulation, Atmos. Chem. Phys., 13, 5227–5241, doi:10.5194/acp-13-5227-2013, 2013.

van der Werf, G. R., Randerson, J. T., Giglio, L., Collatz, G. J., Mu, M., Kasibhatla, P. S., Morton, D. C., DeFries, R. S., Jin, Y., and van Leeuwen, T. T.: Global fire emissions and the contribution of deforestation, savanna, forest, agricultural, and peat fires (1997–2009), Atmos. Chem. Phys., 10, 11707–11735, doi:10.5194/acp-10-11707-2010, 2010.

Walters, D. N., Best, M. J., Bushell, A. C., Copsey, D., Edwards, J. M., Falloon, P. D., Harris, C. M., Lock, A. P., Manners, J. C., Morcrette, C. J., Roberts, M. J., Stratton, R. A., Webster, S., Wilkin-

son, J. M., Willett, M. R., Boutle, I. A., Earnshaw, P. D., Hill, P. G., MacLachlan, C., Martin, G. M., Moufouma-Okia, W., Palmer, M. D., Petch, J. C., Rooney, G. G., Scaife, A. A., and Williams, K. D.: The Met Office Unified Model Global Atmosphere 3.0/3.1 and JULES Global Land 3.0/3.1 configurations, Geosci. Model Dev., 4, 919-941, doi:, 2011.

Ward, D. S., Kloster, S., Mahowald, N. M., Rogers, B. M., Randerson, J. T., and Hess, P. G.: The changing radiative forcing of fires: global model estimates for past, present and future, Atmos. Chem. Phys., 12, 10857–10886, doi:10.5194/acp-12-10857-2012, 2012.

Wilson, D. R. and Ballard, S. P.: A microphysically based precipitation scheme for the UK Meteorological Office Unified Model, Q. J. Roy. Meteor. Soc., 125, 1607–1636, 1999.

Wu, L., Su, H., and Jiang, J. H.: Regional simulations of deep convection andbiomass burning over South America: 2. Biomass burning aerosol effects on clouds and precipitation, J. Geophys. Res.-Atmos., 116, D17209, doi:10.1029/2011JD016106, 2011.

Yu, H., Liu, S., and Dickinson, R.: Radiative effects of aerosols on the evolution of the atmospheric boundary layer, J. Geophys. Res.-Atmos., 107, 4142, doi:10.1029/2001JD000754, 2002.

Zhang, Y., Fu, R., Yu, H., Dickinson, R. E., Juarez, R. N., Chin, M., and Wang, H.: A regional climate model study of how biomass burning aerosol impacts land-atmosphere interactions over the Amazon, J. Geophys. Res.-Atmos., 113, D14S15, doi:10.1029/2007JD009449, 2008.

Zhang, Y., Fu, R., Yu, H., Qian, Y., Dickinson, R., Silva Dias, M. A. F., da Silva Dias, P. L., and Fernandes, K.: Impact of biomass burning aerosol on the monsoon circulation transition over Amazonia, Geophys. Res. Lett., 36, L10814, doi:10.1029/2009GL037180, 2009.

Table 1. Experimental setups using the MetUM model.

Experiment set up	Aerosol Representation
NOA	No Aerosol
CLIM	Direct radiative effect (DRE) from climatological BBA
PROG	DRE from CLASSIC BBA prognostic scheme

Table 2. Mean modelled short-range weather changes with standard deviations (and standard error in brackets) due to BBA in box A (Fig. 1) over day 1 and day 2 of simulations. The net atmospheric divergence is denoted as ATM. NA denotes that data are not available.

Radiation and Weather parameters	PROG-NOA		CLIM-NOA	
	Day 1	Day 2	Day 1	Day 2
All-sky net surface radiation ($W\,m^{-2}$)	-9 ± 1 (0.005)	-11 ± 2 (0.01)	-12 ± 2 (0.01)	-15 ± 3 (0.016)
All-sky net TOA radiation ($W\,m^{-2}$)	-4 ± 1 (0.005)	-5 ± 2 (0.01)	-5 ± 1 (0.005)	-6 ± 2 (0.01)
Clear-sky net surface radiation ($W\,m^{-2}$)	-15 ± 1 (0.005)	-18 ± 1 (0.005)	-19 ± 2 (0.01)	-24 ± 3 (0.016)
Clear-sky net TOA radiation ($W\,m^{-2}$)	-8 ± 1 (0.005)	-10 ± 1 (0.005)	-10 ± 1 (0.005)	-12 ± 1 (0.005)
All-sky ATM ($W\,m^{-2}$)	5 ± 0.4 (0.002)	7 ± 1 (0.005)	7 ± 1 (0.005)	9 ± 1 (0.005)
Clear-sky ATM ($W\,m^{-2}$)	7 ± 1 (0.005)	8 ± 1 (0.005)	9 ± 1 (0.005)	12 ± 2 (0.01)
2 m-Temperature (°C)	-0.1 ± 0.02 (0.0001)	-0.2 ± 0.02 (0.0001)	-0.2 ± 0.03 (0.0002)	-0.3 ± 0.03 (0.0002)
Skin Temperature (°C)	-0.2 ± 0.03 (0.0002)	-0.3 ± 0.03 (0.0002)	-0.3 ± 0.03 (0.0002)	-0.3 ± 0.04 (0.0002)
10 m-wind speed ($m\,s^{-1}$)	-0.03 ± 0.01 (5×10^{-5})	-0.03 ± 0.01 (5×10^{-5})	-0.03 ± 0.01 (5×10^{-5})	-0.03 ± 0.01 (5×10^{-5})
2 m-Relative Humidity (%)	1 ± 0.2 (0.001)	1 ± 0.2 (0.001)	1 ± 0.2 (0.001)	1.1 ± 0.2 (0.001)
Boundary layer depth (m)	-19 ± 8 (0.04)	-24 ± 8 (0.04)	-24 ± 8 (0.04)	-29 ± 8 (0.04)
Rainfall $mm\,day^{-1}$	-0.06 ± 2 (0.01)	0.02 ± 1 (0.005)	-0.05 ± 2 (0.01)	-0.12 ± 1 (0.005)
Atmospheric moisture flux convergence ($mm\,day^{-1}$)	0.1	-0.005	-0.02	0.01
Evapotranspiration ($mm\,day^{-1}$)	-0.2 ± 0.04 (0.0002)	NA	-0.3 ± 0.05 (0.0003)	NA

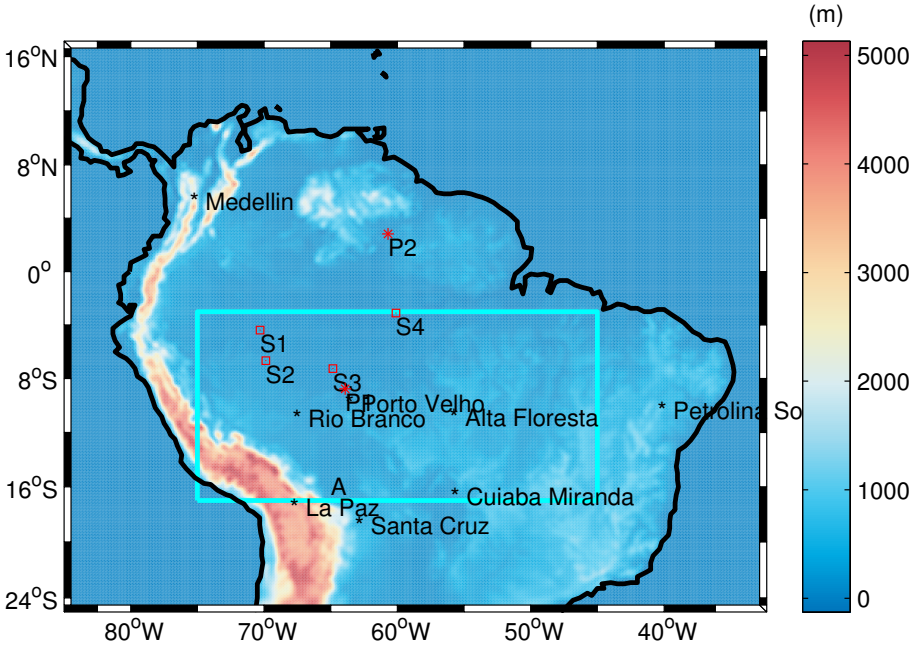

Figure 1. Model domain and orography. Box A (blue) is used to calculate the short-range weather changes due to BBA in Table 2. S1, S2, S3, S4 show locations of surface observations at Benjamin Constant, Eirunepe, Labrea and Manaus, respectively. P1 and P2 are locations of radiosoundings at Porto Velho and Boa Vista. Black asterisks (*) denote AERONET stations.

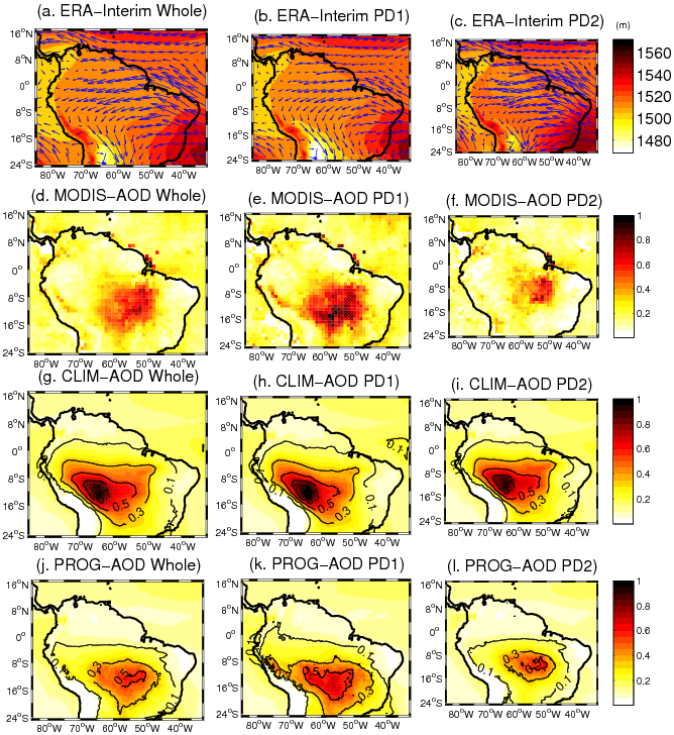

Figure 2. Geopotential height and wind vectors at 850 hPa from ERA-Interim **(a, b, c)** and 550 nm AODs from MODIS **(d, e, f)**, from total AOD in CLIM **(g, h, i)** and total AOD in PROG **(j, k, l)**. Plots are for whole period **(a, d, g, j)**, first period PD1 **(b, e, h, k)**, second period PD2 **(c, f, i, l)**. Contours show BBA AOD.

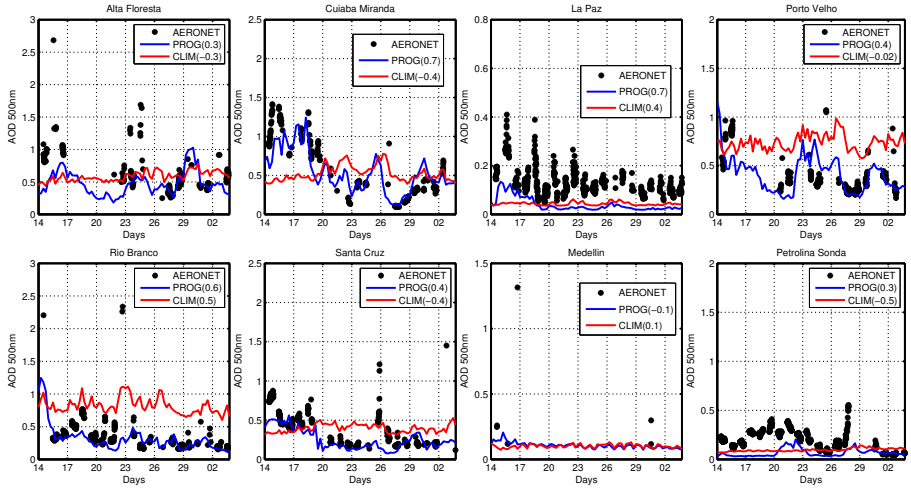

Figure 3. Time series comparison of AERONET (black *), PROG (blue line), CLIM (red line) 550 nm AOD at different locations. Correlation coefficients between AERONET and models are shown in parenthesis.

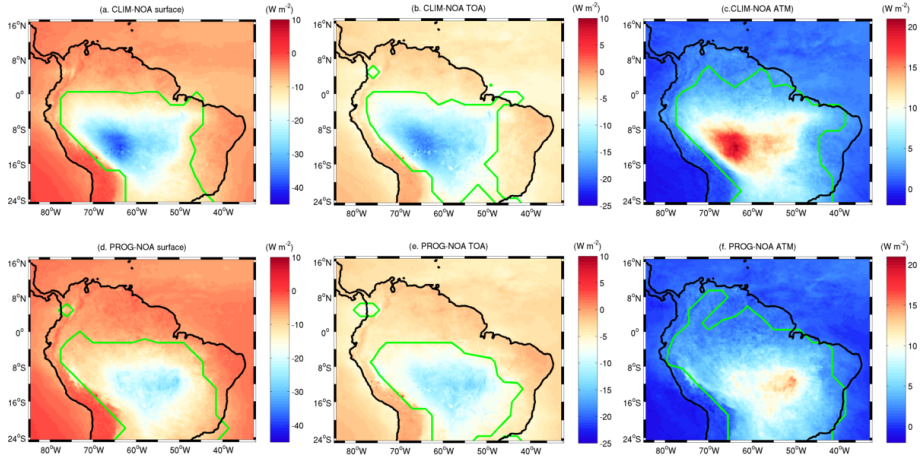

Figure 4. Impact of (top row) CLIM and (bottom row) PROG aerosol representations on **(a, d)** the net surface radiation, **(b, e)** net TOA radiation, **(c, f)** net atmospheric divergence averaged over the whole SAMBBA period for clear-sky. Green contour shows where BBA impacts are greater than the standard error

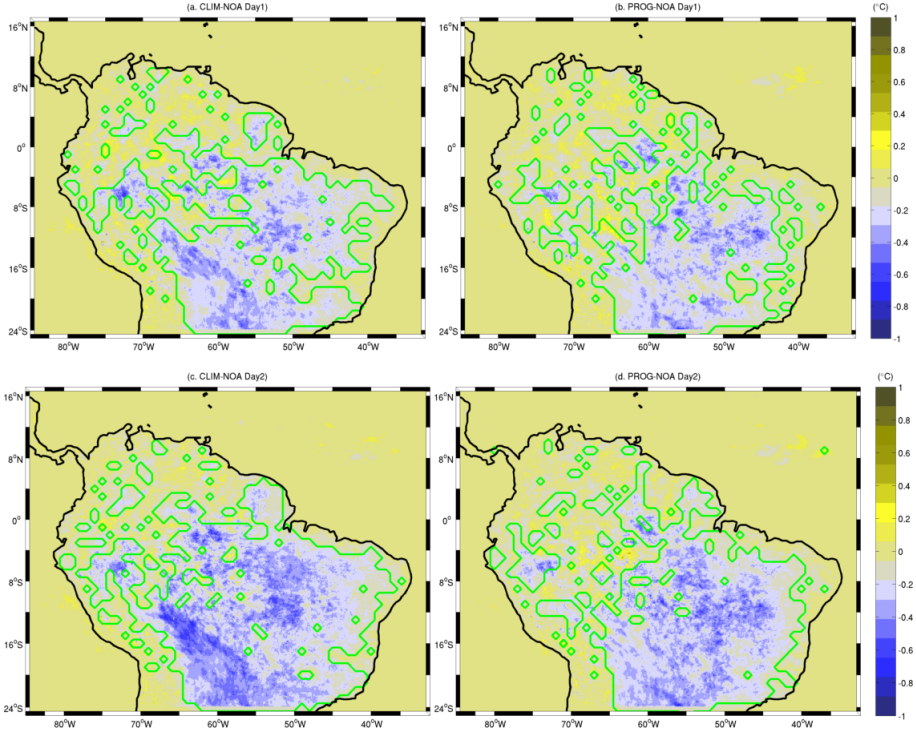

Figure 5. Impact of BBA on 2 m air temperature for day 1 **(a, b)** and day 2 **(c, d)**. Green contour shows where BBA impacts are greater than the standard error.

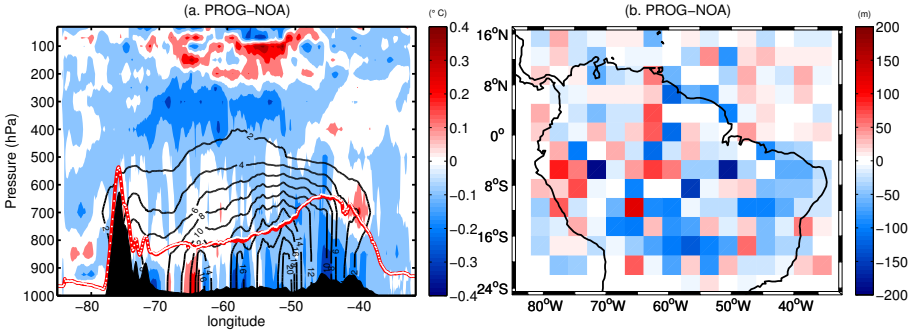

Figure 6. (a) Differences in potential temperature (coloured), BBA mass mixing ratio ($\mathrm{ng\,g^{-1}}$, black contours) averaged over 10–13° S for the entire campaign period at 18:00 UTC for PROG-NOA. Red and white lines are boundary layer depth of PROG and NOA respectively. Topography is masked black. **(b)** Differences in BL height PROG-NOA.

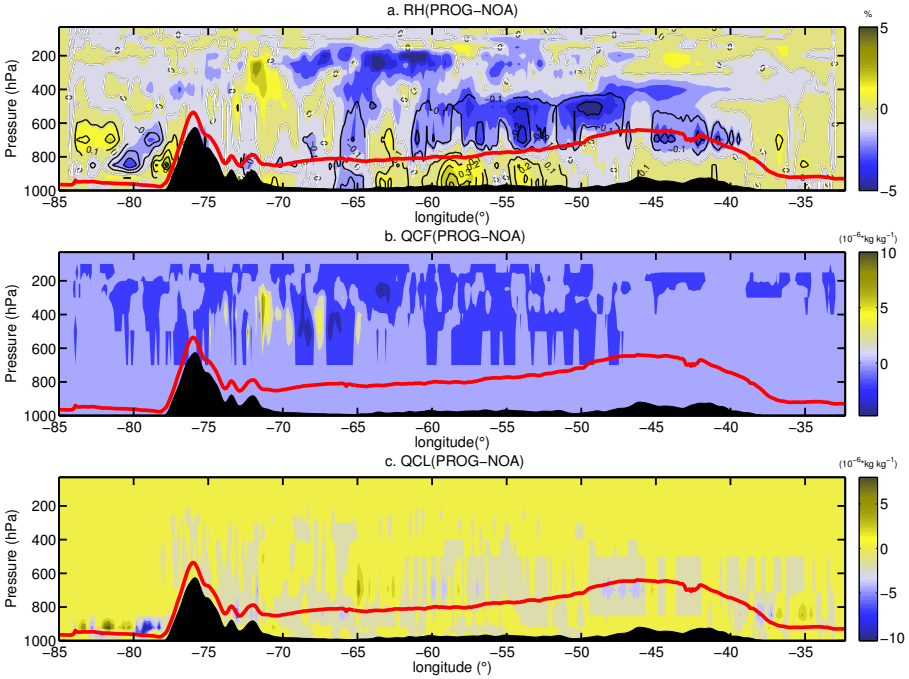

Figure 7. As Fig. 6 but differences are for **(a)** Relative humidity (coloured), black contours are specific humidity (g kg^{-1}), **(b)** Ice cloud water (QCF), **(c)** Liquid cloud water (QCL). Red line is boundary layer depth of PROG. Topography is masked in black.

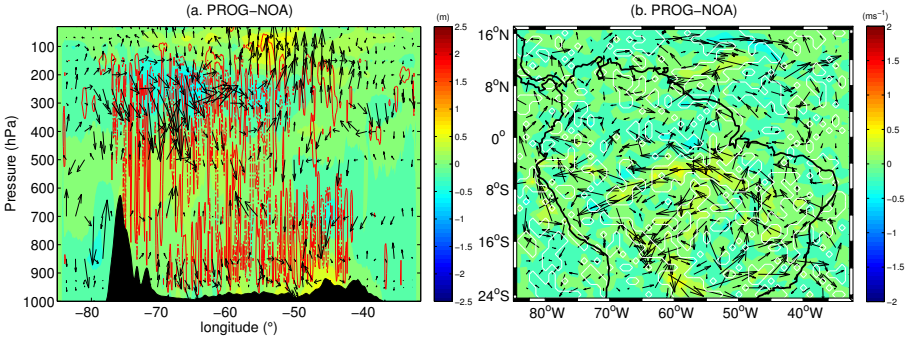

Figure 8. (a) Differences in geopotential height (coloured) and u, v winds (arrows) averaged over 10–13° S for the SAMBBA whole period, for PROG-NOA, red contours show differences in vertical wind(dashed lines show negative values, solid lines positive values). Black masked area is the topography. **(b)** Circulation and wind speed changes at 700 hPa for PROG-NOA.White contour shows where BBA impacts are greater than the standard error.

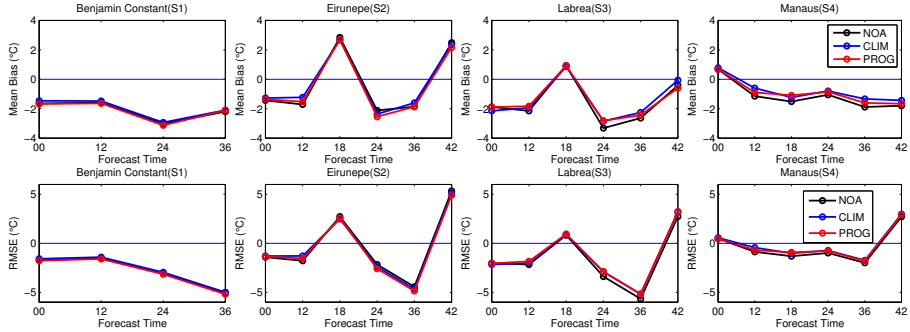

Figure 9. Mean bias and RMS error of modelled temperature at S1, S2, S3 and S4 locations (Fig. 1), averaged over the whole period.

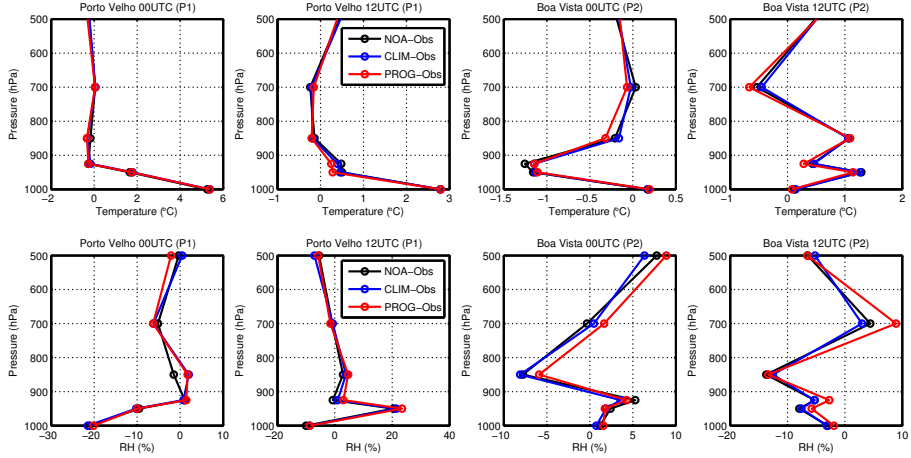

Figure 10. Profiles of modelled minus observed temperature and relative humidities from radiosondes at P1 and P2 (locations shown in Fig. 1).

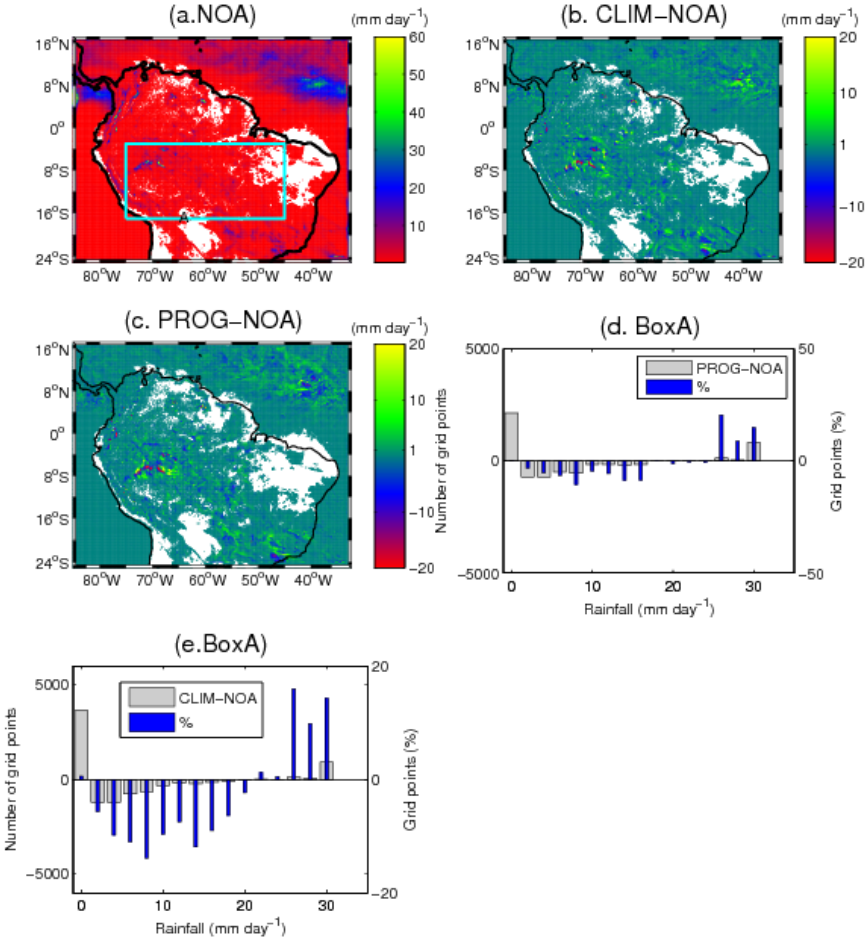
(a.NOA)
(mm day^{-1})
60
50
40
30
20
10
16°N
8°N
0°
8°S
16°S
24°S
80°W 70°W 60°W 50°W 40°W
(b. CLIM–NOA)
(mm day^{-1})
20
10
1
−10
−20
(c. PROG–NOA)
(mm day^{-1})
Number of grid points
(d. BoxA)
PROG–NOA
%
5000
0
−5000
50
−50
Grid points (%)
Rainfall (mm day^{-1})
0
10
20
30
(e.BoxA)
CLIM–NOA
%
Number of grid points
Grid points (%)
Rainfall (mm day^{-1})

Figure 11. The whole SAMBBA period mean rainfall **(a)**, differences in rainfall **(b, c)** , white region shows masked 0 values(a, b, c). and changes to frequency distributions of precipitation **(d–e)** from BBA to NOA for box A. Blue bars are in percentage with respect to differences.